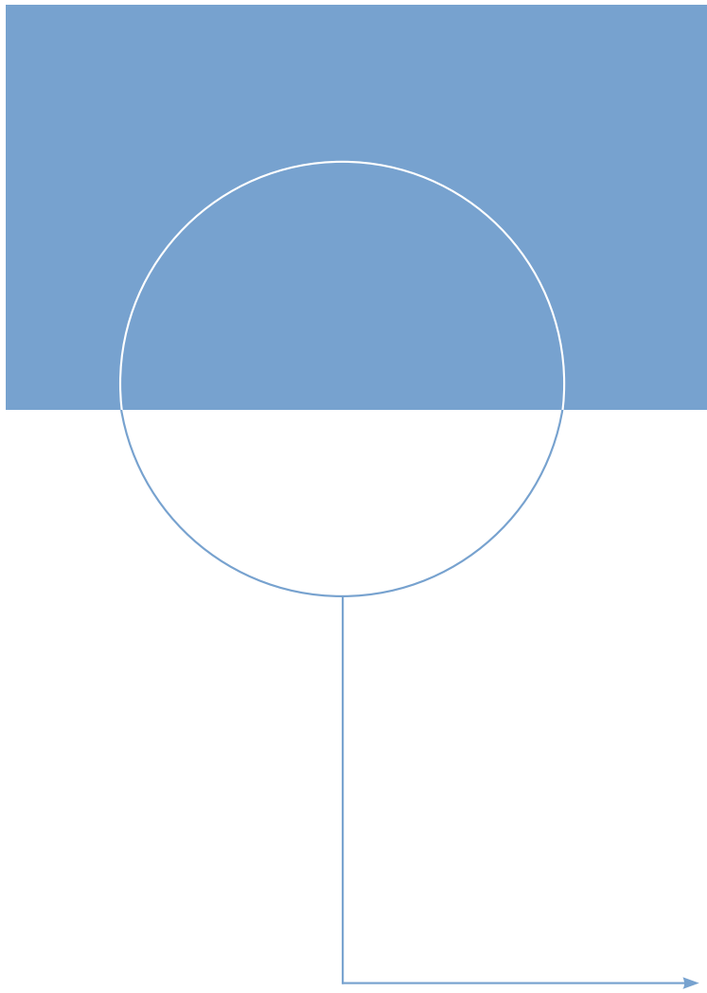

Master's thesis

2019

Sigrid Hoel

NTNU
Norwegian University of
Science and Technology
Faculty of Medicine and Health Sciences
Department of Clinical and Molecular Medicine

Sigrid Hoel

Matrix Metalloproteinase (MMP)-17 Regulates Intestinal Regeneration after Irradiation

June 2019

NTNU
Norwegian University of
Science and Technology

NTNU
Norwegian University of
Science and Technology

NTNU

Norwegian University of
Science and Technology

Matrix Metalloproteinase (MMP)-17 Regulates Intestinal Regeneration after Irradiation

Molecular Medicine
Submission date: June 2019
Supervisor: Menno Oudhoff
Co-supervisor: Mara Martin Alonso

Norwegian University of Science and Technology
Department of Clinical and Molecular Medicine

Abstract

The intestinal epithelium is a multitasking tissue and has a large flexibility to adapt to different types of insults. This is mostly due to the proliferative intestinal stem cells (ISCs) at the bottom of the intestinal crypt, which are highly dependent on cues and signals from surrounding cells. The smooth muscle cells (SMCs) of the muscle layers in the intestine have recently been suggested to act as a possible regulator of ISCs. The SMCs have further been identified to specifically express Matrix Metalloproteinase (MMP)-17, a protease which has been shown to be involved in several diseases and pathologies. However, the role of SMCs and MMP17 in the intestine remains unknown. Here we demonstrate a function of MMP17 during the repair process following the loss of ISCs, caused by radiation exposure. We found that the lack of MMP17 caused impaired regeneration through sustained damaged and structural alterations in the ileum 3 and 6 days after irradiation. We in addition observed a potential decrease of proliferative cells at the bottom of intestinal crypts 6 days after irradiation in mice lacking MMP17. Furthermore, we found that the lack of MMP17 led to a decreased expression of an ISCs marker under homeostatic conditions. With this, our results demonstrate a role for MMP17 in both homeostasis and regeneration following radiation exposure. Furthermore, since the irradiation induces a low inflammatory response, the possibility of MMP17 cleaving substrates important for regulation of the inflammatory response to injury can be rejected. However, further work is needed to specify the substrates and signaling pathways in which this protease interacts. The characterization of MMP17 in the intestine is of high interest, as it could be used as a therapeutic target in gastrointestinal diseases and cancers.

Acknowledgements

This thesis was conducted at the Centre of Molecular Inflammation Research (CEMIR) at St. Olavs University Hospital Trondheim in collaboration with the Oudhoff group.

I first want to thank my principle supervisor Menno Oudhoff, for all the guidance within the field and advice provided throughout my project. Second, I would like to thank my co-supervisor Mara Martin Alonso, for teaching me all the techniques used in the thesis and doing everything possible to help me succeed with this project. I appreciate all the knowledge that you have shared with me throughout the last year and the final product would not have been the same without all your help.

To all the other members of the Oudhoff group – thank you for helping me out whenever needed and for all the input and suggestions around my project. Thank you to everyone working at CEMIR, the Comparative Medicine Core Facility (CoMed) and the Cellular and Molecular Imaging Core Facility (CMIC) for making the completion of this project possible.

Lastly, I want to thank my family and friends for all the support and encouragement throughout this process.

Thank you!

Sigrid Hoel

Table of Contents

List of figures

Abbreviations

BMP	Bone morphogenetic protein
BSA	Bovine serum albumin
CAS3	Cleaved Caspase-3
CBC	Crypt base columnar
DSS	Dextran sodium sulfate
ECM	Extracellular matrix
EGF	Epidermal growth factor
Gy	Gray
H&E	Hematoxylin and eosin
IBD	Intestinal bowel disease
IF	Immunofluorescence
ISC	Intestinal stem cell
ISH	In situ hybridization
LGR5	Leucine-rich repeat-containing G-protein coupled receptor 5
MMP	Matrix metalloproteinase
MT	Membrane-type
NGS	Normal goat serum
NLS	Nuclear localization signal
OLFM4	Olfactomedin-4
PBS	Phosphate-buffered saline
PFA	Paraformaldehyde
SEM	Standard error of the mean
SMC	Smooth muscle cells
TA	Transit amplifying
TBST	Tris-buffered saline and Tween
TGF	Transforming growth factor
UEA-1	Ulex Europaeus Agglutinin 1
WNT	Wingless-type MMTV integration site family member

1 Introduction

1.1 The intestine

The human intestine contains the second largest epithelium in the human body and it is a true multitasking tissue. It must simultaneously achieve efficient digestion and absorption of nutrients and water from foods and liquids, while providing an effective barrier against the harsh environment present in the intestinal lumen. These features of the intestine are possible because of its distinct organization and structure.

The mucosa in the intestine consist of a single layer of epithelium, the underlying connective tissue called lamina propria and lastly the muscularis mucosae. The mucosa has three main functions; absorption, secretion and protection (Rao & Wang, 2010). The lamina propria is underneath the epithelium and consists of immune cells, mesenchymal-, endothelial- and nerve cells. The muscularis mucosae is composed of a layer of smooth muscle cells (SMCs) and the exact function of this muscle layer is uncertain, but it has been assumed to exclusively provide contractile functions during digestion (Chivukula et al., 2014). The submucosa is underneath the mucosa and is a dense layer of connective tissue (Ross & Pawlina, 2016). Under the submucosa is the muscularis externa, which contains two thick layers of smooth muscle and its contraction determine the intestinal movement of segmentation and peristalsis (Ross & Pawlina, 2016). The intestine also contains a branching network of nerves, called nervous plexus, one in the submucosa and one between the muscles in the muscularis externa (Ross & Pawlina, 2016). The different layers in the intestine are illustrated in Figure 1-1.

Throughout the intestine the mucosa creates a barrier between the exterior and the interior through the single-layer of epithelial cells. The epithelial lining structure varies throughout the different parts of the gastrointestinal tract. The small intestine, making up the first part of the digestive tract after the stomach, is divided into the duodenum, jejunum and ileum (Rao & Wang, 2010; Ross & Pawlina, 2016). The main task of the small intestine is to digest food and to mediate the absorption of the products from digestion. Here, the epithelium forms finger-like projections into the intestinal lumen, called villi (Ross & Pawlina, 2016). These structures greatly increase the absorptive surface and thereby the absorptive ability of the small intestine. Each villus is enriched in tubular invaginations of the epithelium (Rao & Wang, 2010; Ross & Pawlina, 2016). These structures are referred to as intestinal crypts, crypts of Lieberkühn, intestinal glands or just crypts. The large intestine is the distal part of the gastrointestinal tract

and is composed of the cecum, the colon, the rectum and the anal canal (Rao & Wang, 2010; Ross & Pawlina, 2016). The colon is the largest portion, so the large intestine is often referred to as the colon and vice versa. In humans it is divided into the proximal (ascending) part and the distal (descending) part (Rao & Wang, 2010). The large intestine is responsible for the reabsorption of electrolytes and water and the elimination of undigested food and waste. The epithelial lining of the colon is completely "smooth", due to the absence of villi, and here the epithelium is only organized into crypts (Ross & Pawlina, 2016). The organization of the small- and the large intestine is illustrated in Figure 1-1.

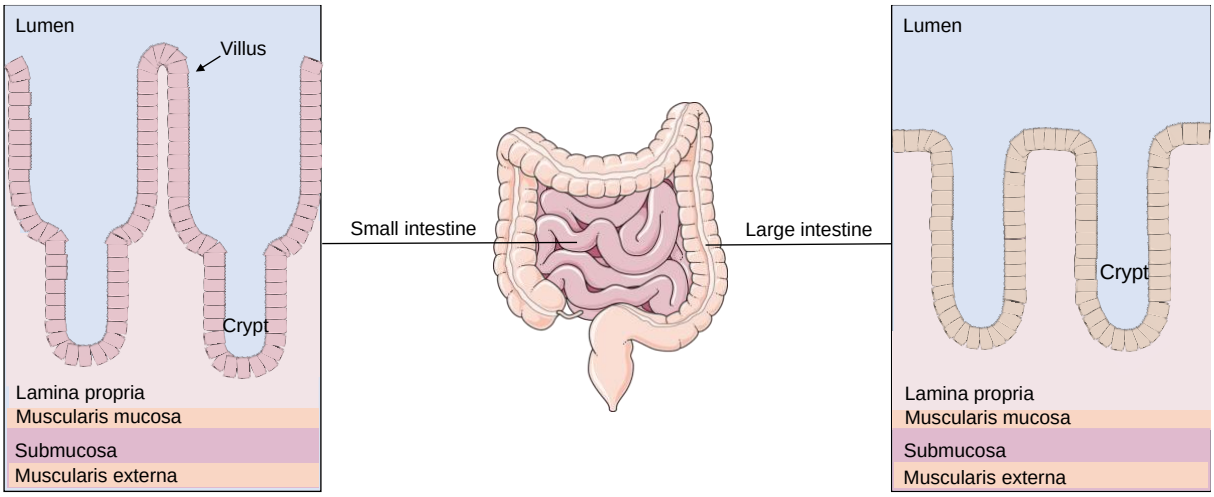

Figure 1-1: Organization of the intestinal epithelium. The epithelium in the small intestine is organized into crypt-villus structures. The epithelium in the colon is organized into a flat structure enriched in crypts. The epithelium in both parts of the intestine is supported by underlying structures; lamina propria, muscularis mucosa, submucosa and muscularis externa. (Images retrieved from Servier Medical Art).

1.2 The intestinal crypt

As mentioned earlier, the intestinal crypts are invaginations of the epithelial monolayer into the lamina propria and down close to the muscularis mucosae. An illustration of the intestinal crypt in the small intestine is shown in Figure 1-2. At the bottom of the crypt, well protected from the hazardous contents of the lumen, is where the intestinal stem cells (ISCs) reside. These ISCs are characterized by their ability to self-renew and the ability to generate all differentiated cell linages; the two characteristics that are necessary for being classified as an adult somatic stem cell (Wagers & Weissman, 2004). A population of ISCs occupying the far bottom of the crypt, called crypt base columnar (CBC) cells, was identified in 1974 (Cheng & Leblond, 1974). They were described as undifferentiated, mitotically active and phagocytotic cells back then, but they

failed to gain full acceptance as an adult stem cell. This changed in 2007 when the Wingless-type MMTV integration site family member (WNT) target gene *Leucine-rich repeat-containing G-protein coupled receptor 5 (Lgr5)* was identified as a genetic marker for this type of stem cell, allowing further characterization of these ISCs and classifying them as active somatic stem cells (Barker et al., 2007). For the rest of this text, ISCs will refer to proliferative and active CBC cells.

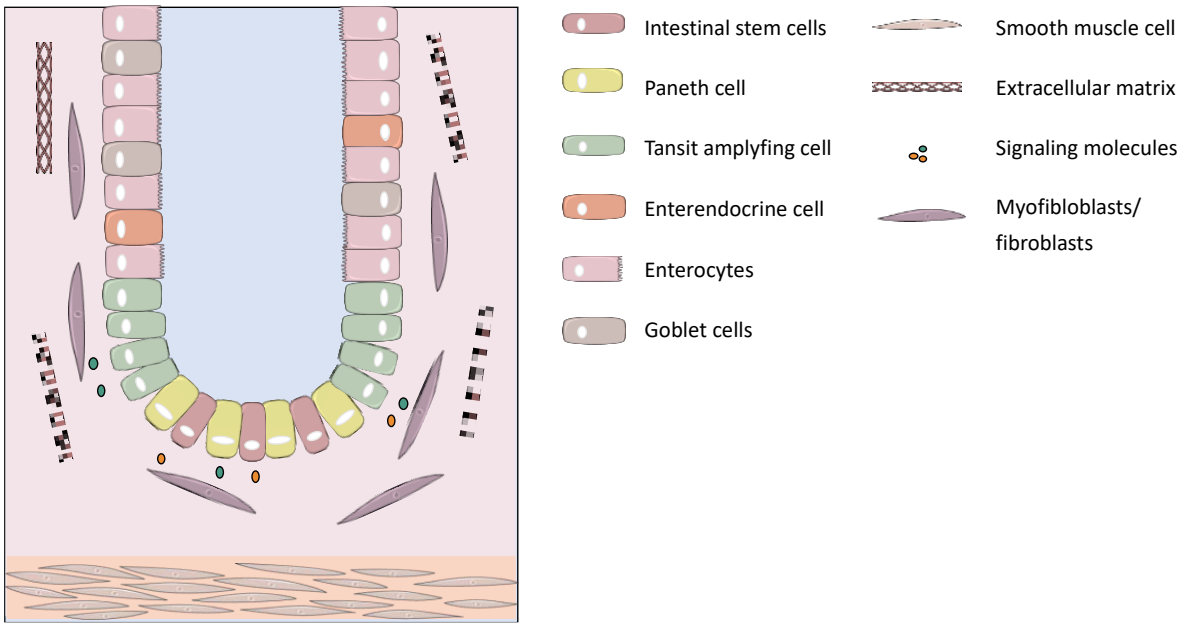

Figure 1-2: Overview of the intestinal crypt in the small intestine. Intestinal stem cells (ISCs) reside at the bottom of the crypt, interspaced between Paneth cells. They divide giving rise to transit-amplifying (TA) daughter cells that differentiate to the distinct epithelial cell linages; enteroendocrine-, enterocyte-, Paneth- and goblet cells. The epithelial and surrounding cells make up the microenvironment around the ISCs. The surrounding cells in the lamina propria are myofibroblast/fibroblasts and smooth muscle cells (SMCs) of the muscularis mucosae. These cells are responsible for producing and reorganizing the extracellular matrix (ECM) in the lamina propria. (Images retrieved from Servier Medical Art).

ISCs are continuously dividing, giving rise to transit amplifying (TA) daughter cells. While migrating up along the crypt away from the stem cell zone, the TA cells differentiate into the different epithelial lineages found in the intestinal epithelium; the secretory linage and the absorptive linage.

The secretory linage includes goblet-, Paneth- and enteroendocrine cells. Goblet cells are responsible for secreting mucins, which forms a protective coat of mucus along the epithelium (Milano et al., 2004; van Es et al., 2005; VanDussen & Samuelson, 2010). In contrast to the other epithelial cells, Paneth cells are only present in the small intestine and they are the only epithelial cells that move downwards, towards the ISCs, during differentiation (Batlle et al.,

2002; Genander et al., 2009). Here they are interspaced between ISCs and provide necessary signals and growth factors for the ISCs (Farin et al., 2012; Sato et al., 2010). This will be discussed in further detail in section 1.2.1. In addition, Paneth cells produce a wide variety of antimicrobial products, that together with the mucus from goblet cells, form a part of the mucosal immunity along the epithelium (Allaire et al., 2018). Enteroendocrine cells produce and release several paracrine and endocrine hormones upon stimulation and are divided into several subtypes based on the specific hormones they secrete (Gehart & Clevers, 2019).

The absorptive lineage is only composed of one cell type, the enterocyte. It is one of the most abundant cell types in the intestinal epithelium. They are responsible for the uptake of ions, water, carbohydrates, peptides and lipids from the intestinal lumen and transport of these into the circulatory system (Gehart & Clevers, 2019).

As the epithelial cells divide, excluding the Paneth cells, they are pushed up towards the top of the crypt in the colon or the villus tip in the small intestine. Here, they eventually go through a type of programmed cell death, called anoikis, where they are detached from the surrounding extracellular matrix (ECM) and shed into the lumen (Barker, 2014). This process takes between 3-5 days and makes sure that only post-mitotic epithelial cells are exposed to the hazardous environment of the intestinal lumen, since the epithelial population is consistently replenished by the dividing ISCs at the bottom of the crypt (Barker, 2014). The crypt is therefore a highly dynamic structure, where there is a constant need of surrounding cells to supply necessary signals and factors to maintain and tightly regulate the ISCs, making up the ISC niche (see section 1.2.1)

Another subtype of the ISC population have been described, called +4 cells. The "+4" describes the cells location, 4 cells above the bottom crypt cell and just above the upper Paneth cell. It was identified by Chris Potten (Potten et al., 1978; Potten et al., 2002) and later research have identified several genetic markers for this population; *Bmi1* (Sangiorgi & Capecchi, 2008), *Tert* (Breault et al., 2008; Montgomery et al., 2011), *Hopx* (Takeda et al., 2011) and *Lgr1* (Powell et al., 2012). There is still much controversy and debate surrounding +4 cells' role as a stem cell in intestinal homeostasis, but its role in regeneration has been well documented (Breault et al., 2008; Montgomery et al., 2011; Powell et al., 2012; Sangiorgi & Capecchi, 2008; Takeda et al., 2011). It has been considered to function as a "reserve" stem cell with high resistance to radiation due to their slow-cycling nature and that they are able restore the pool of bottom ISCs when needed (Tian et al., 2011), but its radiation sensitivity has been debated (Metcalfe et al.,

2014). Furthermore, research focusing on regeneration and plasticity of the intestinal epithelium places the existence of a specific reserve stem cell into question. It is debated that the regeneration of the epithelium is far more dynamic and that other epithelial cells can de-differentiate and replenish the ISCs pool under certain circumstances (Asfaha et al., 2015; Buczacki et al., 2013; Schmitt et al., 2018; Tetteh et al., 2016; van Es et al., 2012; Yu et al., 2018).

1.2.1 The intestinal stem cell niches

A niche can be defined as a specialized instructive microenvironment necessary to maintain and regulate stem cell self-renewal and proliferation (Barker, 2014). The niches in the crypt can be divided into two distinct parts. First, the cellular niche, which contains the cells in the stromal microenvironment around the ISCs and the epithelial cells. Second, the physical niche, which refers to the ECM, a network of fibrous structural proteins created by surrounding cells.

There are several main niche factors that are highly important for proper ISC function and one of them are WNT ligands. The WNT pathway plays a crucial role in development and maintaining the proliferative capacity of the ISCs (Nusse & Clevers, 2017). A second main niche component is epidermal growth factors (EGFs), which binds to EGF receptors expressed on ISCs and helps to control their division rate (Sato et al., 2010). Notch ligands in the intestinal niche are responsible for inhibiting and blocking differentiation of ISCs into the secretory lineage (Sancho et al., 2015). Lastly, bone morphogenetic proteins (BMP) are a group of growth factors that belong to the transforming growth factor-β (TGF-β) superfamily, that promotes differentiation of ISCs (He et al., 2004). A gradient of these main niche factors assures high proliferative activity at the bottom of the crypt and aids differentiation of cells towards the top of the crypt and villus.

As mentioned, Paneth cells are found interspaced between ISCs at the bottom of the crypt. They provide important niche signals through secreting soluble factors and membrane-anchored factors. They secrete WNT3, which is the main WNT ligand regulating ISC self-renewal and proliferation. (Alexandre et al., 2014). Paneth cells also secretes EGFs (Sato et al., 2010) and Notch ligands (Sancho et al., 2015).

Paneth cells are not the only cell contributing to the ISCs niche, other growth factors responsible for ISC regulation are produced by mesenchymal cells. The term “mesenchymal cells” refers

to cells of the intestinal lamina propria that are non-hematopoietic, non-epithelial and non-endothelial, like intestinal fibroblasts, myofibroblasts, pericytes, smooth muscle cells of the muscularis mucosae and mesenchymal stromal/stem cells. Fibroblasts and myofibroblasts are the major two cell types in the lamina propria in the intestine. Fibroblasts are in part responsible for synthesizing the ECM and collagen, contributing to the structural framework in tissues and they have been shown to play a critical role in wound healing. During wound healing fibroblasts can differentiate into myofibroblasts, an intermediate cell between fibroblasts and SMCs (Desmouliere et al., 2005). In addition, it has been shown that mesenchymal cells in the small intestinal villi and the sub-epithelial mesenchyme in colon express non-canonical WNT molecules (WNT2B, WNT4, WNT5A and WNT5B) (Gregorieff et al., 2005). Pericryptal myofibroblasts also support the ISCs niche, producing different factors such as WNT ligands and BMP antagonists (Meran et al., 2017). And although SMCs have not been considered as contributing members to the ISC niche, research shows that they express BMP antagonists *Germlin 1, Gremlin 2 and Chordin-like 1* in the human colon (Kosinski et al., 2007). BMP antagonists bind and block different members of the BMP family, important in maintaining the highly proliferative, self-renewal activity of ISCs at the bottom of the crypt (He et al., 2004; Kosinski et al., 2007; Stzepourginski et al., 2017).

Other cell types have also been shown to contribute to the cellular niche. Neural cells are the main component of the nervous tissue and have been shown to be important in intestinal epithelial growth (Bjerknes & Cheng, 2001) and to exert protective functions during inflammation and injury by secretion of EGF and TGF-β isoforms (Neunlist et al., 2007; Van Landeghem et al., 2011). Endothelial cells line the interior surface of blood- and lymphatic vessels. It appears that the endothelial cells present in the intestinal lamina propria are important in maintaining epithelial homeostasis, because radiation-induced injury triggers rapid endothelial loss prior to epithelial death (Owens & Simmons, 2013; Paris et al., 2001).

The ECM, making up the physical niche, mainly acts as a scaffold to maintain the three-dimensional shape of tissues, but it is extremely versatile and performs many other functions. As a major part of the microenvironment of cells, the ECM can influence many cellular behaviors, including migration, growth, differentiation and cell death. The lamina propria around the crypts has been reported to be enriched in different ECM components, like fibronectins, laminins, collagens, glycosaminoglycans and integrins, suggesting that these components have a potential role in ISC regulation (Meran et al., 2017).

The biomechanical role of the ECM is thought to influence a wide range of cellular activities. The biomechanical factors include cell shape and ECM stiffness. The cells are able to sense and regulate the ECM mechanics through mostly integrins, that mediate the signaling between the intracellular cytoskeleton and the surrounding ECM structures (Humphrey et al., 2014). Fibroblasts, smooth muscle cells and epithelial cells are very sensitive to mechanical stimuli and can induce matrix stiffness (Chiquet et al., 2009; Peyton & Putnam, 2005). Matrix stiffness is important because it has been shown to influence and regulate cell migration (Pelham & Wang, 1997; Plotnikov et al., 2012), cell cycle progression (Klein et al., 2009), gene expression and cell fate (Engler et al., 2006). Additionally, it has been shown that the ECM can reprogram ISCs after damage, via activation of Hippo transducers Yap/Taz through ECM remodeling (Yui et al., 2018).

In addition, the ECM can act as a ligand "reservoir", through binding of several different growth factors and limit or modify their diffusive range and accessibility. The ECM has been shown to be important in creating concentration gradients of BMP, WNTs and TGF-β (Hynes, 2009; Rozario & DeSimone, 2010). The effectiveness of the ECM, in context of cellular response to injury, is dependent on degradation and remodeling of its structural components.

1.3 Intestinal homeostasis and regeneration after injury

One of the main functions of the intestinal epithelium is to provide protection from commensal and pathogenic microorganisms to the underlying tissues. The key factor to maintaining tissue homeostasis is how the epithelial layer senses and responds to microbial stimuli, reinforcing the physical and biochemical barriers and activating the appropriate immune responses (Peterson & Artis, 2014). The disruption of this barrier, exposes the underlying tissues to these microorganisms, leading to exacerbated mucosal immune responses. There has been an increasing recognition of an association between disrupted intestinal barrier function and the development of autoimmune and inflammatory diseases, including inflammatory bowel disease (IBD) (Heyman, 2005; Heyman & Desjeux, 2000; Mankertz & Schulzke, 2007; Takeuchi et al., 2004). IBD comprises to major phenotypes, Crohns disease and ulcerative colitis, that both are characterized by a continuous cycle of mucosal injury, with an exacerbated mucosal immune response to microbial factors (Clayburgh et al., 2004).

1.3.1 Models of intestinal damage

One of the most widely used animal models to study intestinal damage is the administration of dextran sodium sulfate (DSS) to mice. DSS only affects the colon in mice by not fully understood mechanisms. As mentioned, IBD, which comprises ulcerative colitis and Crohn's disease, are characterized by both acute and chronic inflammation of the intestine with multifactorial etiology (Xavier & Podolsky, 2007). The most severe murine colitis, from administration of DSS (40-50kDA) in drinking water, most closely resembles human ulcerative colitis (Okayasu et al., 1990). The exact mechanisms behind DSS inducing intestinal inflammation are unclear, but it is most likely due to damage of the colonic epithelial monolayer, allowing the dissemination of proinflammatory intestinal contents into the underlying tissue. Acute, chronic and relapsing models of intestinal inflammation can be achieved by modifying the concentration of DSS in the drinking water and the frequency of administration (Chassaing et al., 2014).

A second injury model of intestinal damage is the use of ionizing irradiation in mice, which is used to target mitotically active cells, like ISCs and their dividing progenitor cells (Blanpain et al., 2011; Hendry & Potten, 1974; Potten, 1977). This occurs through DNA damage induced by free radicals causing double-strand breaks (Lewanski & Gullick, 2001). This injury model allows us to study the intestinal capacity for repair after the loss of ISCs. Surprisingly, it has been demonstrated that the gut can recover from doses of radiation that eliminates the proliferative cells in the intestinal crypt (Potten, 1977). The irradiation model also allows us to study how the loss of ISCs at the bottom of the crypts are replenished by other cellular types, as previously mentioned (Asfaha et al., 2015; Buczacki et al., 2013; Schmitt et al., 2018; Tetteh et al., 2016; van Es et al., 2012; Yu et al., 2018).

While both the small and large intestine have similar organization and underlying mechanisms, the colonic ISCs have unexpectedly been shown to beq more resistant to ionizing radiation. It has been reported that colonic ISCs survived an exposure of 30 Gray (Gy), while ISCs in the small intestine were completely depleted after 15 Gy (Hua et al., 2017). However, both in the small intestine and the colon, the regenerative response after radiation exposure can be divided into the three distinct phases. The first phase is an injury phase that occurs within hours after radiation exposure and lasts around 48 hours (Kim et al., 2017). During this phase the ISCs die and as a result, irradiated intestine shows crypt loss, shrinkage in crypt size, apoptotic cells at the bottom of the crypts and shortening of the villi (Booth et al., 2012; Merritt et al., 1994). The

shortening of the villi, also called villus blunting, is a non-specific reaction of the mucosae, which can occur under various insults. It is due to the hyper-elongation or hypo-regeneration of crypts (Serra & Jani, 2006). During the injury phase the ECM goes through degradation and reorganization. The next phase, known as the regenerative phase, occurs two to four days post-radiation (Kim et al., 2017). During this phase the surviving crypt cells generates new crypts through crypt fission and proliferate to restore the pool of $Lgr5^+$ ISCs, which is described in more detail in the next section (1.3.2). The number of crypts is decreased, and crypts are enlarged in length due to the increased proliferation occurring in this phase (Kim et al., 2017). This elongation of the crypt will also reduce the crypt to villus ratio (Serra & Jani, 2006). Also, the ECM suffers changes and remodeling to complete mucosal healing. In the last "normalizing" phase, the size of the crypt and the length of the villi are restored to values similar to homeostatic conditions (Withers et al., 1970; Withers & Elkind, 1970). The three phases after irradiation injury are shown in Figure 1-3.

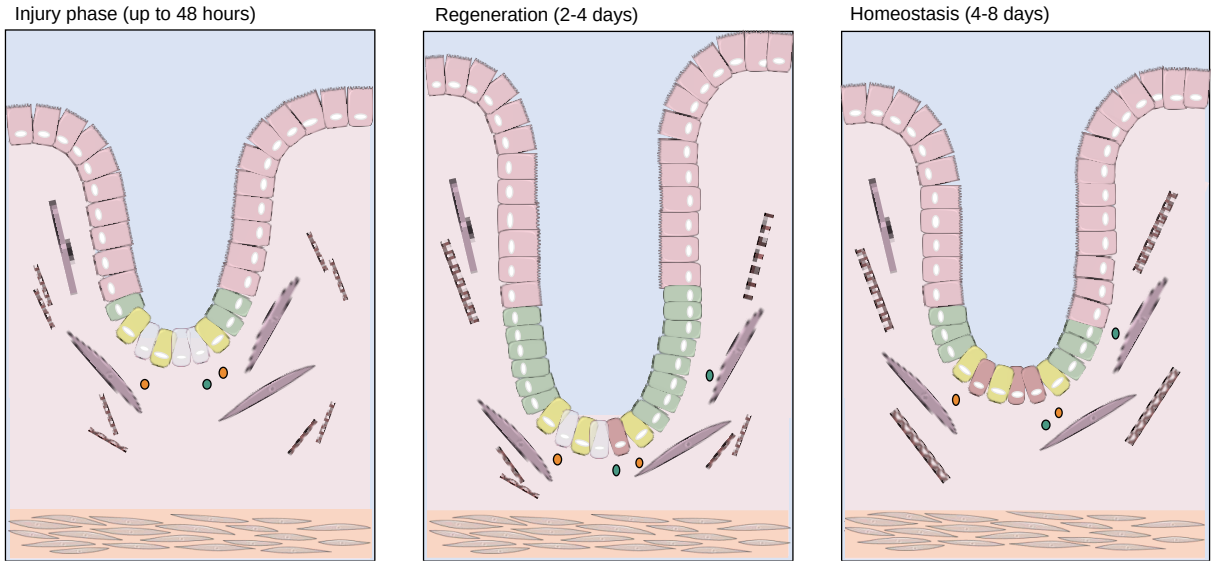

Figure 1-3: The phases after radiation damage in the intestine. Immediately after irradiation the crypt enters an injury phase that lasts for up to 48 hours, where highly dividing cells go through apoptosis and the crypt and villus shrinks in size. Also, in this phase the extracellular matrix (ECM) will be degraded and reorganized. Two to four days post-irradiation the crypt enters a regeneration phase. Here the crypts are enlarged, due to a boost in proliferation of the surviving cells. Eventually, the crypt will regenerate completely and enter a homeostatic phase. (Images retrieved from Servier Medical Art).

1.3.2 Regeneration after injury

The intestinal mucosa can be damaged by mechanical, toxic and/or microbiological insults, as described by the injury models above. The reestablishment of homeostasis and healthy mucosa depends on the crypt cells ability to regenerate and achieve normal architecture after the

damage. The regenerative process after injury is mainly mediated by continuous cell proliferation within the crypt and crypt fission (Bloemendaal et al., 2016; Kim et al., 2017).

As described earlier, the continuous cell proliferation within the crypt is due to the rapidly dividing ISCs at the bottom of the crypt, specifically marked by the gene *Lgr5*. When damage occurs, the proliferative activity boosts in the crypt, reestablishing the continuity of the epithelium by the migration of adjacent and newly divided epithelial cells, keeping the epithelial barrier intact (Kim et al., 2017). The crypt is a dynamic compartment, illustrated by the fact that ablation of *Lgr5*$^{+}$ ISCs does not disrupt intestinal homeostasis (Tian et al., 2011), further demonstrating the plasticity existing within the crypt compartment. As discussed earlier, several cells have been identified to have the ability to replenish the ISC pool after various insults (Asfaha et al., 2015; Buczacki et al., 2013; Schmitt et al., 2018; Tetteh et al., 2016; van Es et al., 2012; Yu et al., 2018).This highlights that plasticity within the crypt is a key mechanism in the intestinal epithelium, making it able to cope with the insults that compromise the ISC compartment.

Crypt fission also contributes to restore tissue homeostasis after injury through the generation of new crypts (Withers & Elkind, 1970). The process was described and identified in more detail in the paper by Miyoshi et al (Miyoshi et al., 2012). After mucosal damage, a layer of non-proliferative epithelial cells (wound-associated epithelial cell) migrates from intact adjacent crypts and floods over the wound-bed surface. Thereafter, adjacent crypts to the wound-bed starts forming an array of channel like structures, which contain highly proliferative cells, from which new crypts arise (Miyoshi et al., 2012) It was also identified that this was a WNT5B dependent process, expressed by mesenchymal cells associated with the wound channels, and necessary to activate TGF-β signaling (Miyoshi et al., 2012).

The processes of increased cell proliferation and crypt fission after intestinal injury are highly dependent on the dynamic interactions in the mucosa, between the ISCs, the epithelial cells and the surrounding cells in the lamina propria. Studies have highlighted the importance of mesenchymal cells in regeneration; CD34^{+} gp38^{+} cells in the mesenchyme were identified to be major sources of GREMLIN1, R-SPONDIN1 and WNT2B, as well as secreting chemokines, cytokines and growth factors, all playing essential roles in gut inflammation and repair (Stzepourginski et al., 2017). In addition, these cells remained associated with the crypts after DSS treatment, indicating their importance in regulation of the ISC niche during repair. Another study demonstrated that SMCs and myofibroblasts could contribute to the injury

response. In this study the lack of miR-143/145 expression by SMCs and myofibroblasts, causing their dysfunction, dramatically impaired the epithelial regeneration after DSS induced injury (Chivukula et al., 2014). This was due to impaired release of growth factors by these cells after DSS. These studies demonstrate the importance of the cross-talk between the mesenchyme and the cells within the crypt during regeneration and repair.

1.4 Matrix metalloproteinases

As mentioned earlier, the ECM is degraded and reorganized as part of the response to damage and injury. The Matrix Metalloproteinase (MMP) family is collectively capable of cleaving all kinds of ECM proteins, contributing to their remodeling and degradation. This family of calcium-dependent zinc-containing endopeptidases includes more than 20 members and the founding member of the family, collagenase, was already identified in 1962 (Gross & Lapiere, 1962).

The MMP family is normally divided into two distinct groups; the group of soluble MMPs (MMP1, -2, -3, -7, -8, -9, -10, -11, -12, -13, -19. -20, -21, -22, -27 and 28) and the group of membrane-type MMPs (MT-MMP). MT-MMPs are divided into the ones bound to the membrane by a transmembrane domain (MMP14, -15, -16 and -24) and the ones attached to the plasma membrane by a GPI anchor (MMP17 and -25) (Yip et al., 2019).

The metalloproteinase part of the MMP name is due to the presence of a zinc cation on their catalytic domain. In general, all of them act as endopeptidases and share a conserved domain structure, consisting of at least a catalytic domain, a signal peptide and an autoinhibitory pro-domain, which interacts with a zinc ion on the catalytic domain (Yip et al., 2019). MMPs are synthesized as these inactive zymogens and requires proteolytic cleavage of their pro-domain to become active (Sternlicht & Werb, 2001). This cleavage of the pro-domain can occur extracellularly, by other MMPs or could be mediated by several serine proteinases (Nagase & Woessner, 1999), or intracellularly, usually by furin (Pei & Weiss, 1995). Most MMPs also contain a hemopexin domain, connected to their catalytic domain by a flexible hinge region, which is important in protein-protein interactions and mediates proper substrate recognition and localization, internalization and degradation (Overall, 2002; Page-McCaw et al., 2007).

MMPs functions were thought to only involve degradation of structural components of the ECM; therefore, they have been classified on the basis of their specificity for these ECM

components in collagenases, elastases et cetera (Page-McCaw et al., 2007; Verma & Hansch, 2007). However, the function of MMPs is not only limited to degradation of the ECM, they can also cleave other proteins such as membrane receptors, signaling molecules, growth factors, other MMPs and proteases (Page-McCaw et al., 2007). This wide array of substrates reflect the biological processes MMPs can regulate, like cell migration, regulation of tissue architecture and numerous signaling pathways (Sternlicht & Werb, 2001).

MMPs have since their discovery gained a lot of interest due to their upregulation in several human diseases, including cancers and inflammatory diseases like rheumatoid arthritis (Brinckerhoff & Matrisian, 2002; Chabottaux & Noel, 2007). Different therapies have been developed to target MMP activity, including both natural and synthetic inhibitors (Coussens et al., 2002; Whittaker et al., 1999). However, no one has so far found a good way to produce and use a chemical that specifically blocks MMPs and that at the same time gives a clinical benefit without any adverse side effects (Cathcart et al., 2015). The lack of knowledge about the different MMPs, their expression, functions and substrates, are the main reasons why no efficient therapies have emerged. In addition, the role MMPs play in pathologies can be dynamic and complex; for example, increased activity of MMP can enhance tumor progression or it can inhibit it, depending on the substrate specificity/location or cell type expression (Lu et al., 2011).

The development of genetic knockout mouse models of MMPs (*Mmp*$^{-/-}$) has opened a valuable opportunity to identify the essential functions and substrates of different MMPs. Surprisingly, all knockout models have shown subtle phenotypes, with all models surviving birth (Page-McCaw et al., 2007). Possible explanations for these subtle phenotypes of the MMP knockout models are enzymatic redundancy, compensation and adaptive development or that MMPs are not necessary until after embryonic development (Page-McCaw et al., 2007). With the development of *Mmp*$^{-/-}$ models, it has been possible to study the role of these proteins in intestinal homeostasis and pathologies. For example, MMP15 was identified as a regulator of apical junction signaling and epithelial cell homeostasis through cleaving E-cadherin (Gomez-Escudero et al., 2017). MMP7 have also shown to be secreted by Paneth cells and capable of activating α-defensins in the intestine (Ayabe et al., 2002). In a number of IBD studies, an upregulation of several different MMPs have been detected, including MMP2, -3. -7 and -9 (Jakubowska et al., 2016; Silosi et al., 2014), indicating the importance of these proteins in intestinal pathologies, which needs to be further analyzed.

1.4.1 Membrane type 4-matrix metalloproteinase

MMP17, also known as MT-MMP 4, was originally discovered in human breast carcinoma (Puente et al., 1996). Since then several studies have shown MMP17 connection to other pathological conditions, however there is still a lack of knowledge concerning MMP17 compared to other MMPs (Sohail et al., 2008).

MMP17 contains the common structures of the MMP family; a signal peptide (also called pre-domain), which drives MMP to the endoplasmic reticulum, a pro-domain, a catalytic domain and a hemopexin domain with a hinge region. In addition, MMP17 contains a GPI anchor and a furin site (R-X-K/R-R) (Yip et al., 2019). The GPI anchor, also present in MMP25, facilitates membrane attachment (Sohail et al., 2008). The structure of the MMP17 protein is shown in Figure 1-4. MMP17's catalytic domain displays less than 40% amino acid sequence identity to the other MMPs, which makes it a distant member of the MMP family (Itoh et al., 1999).

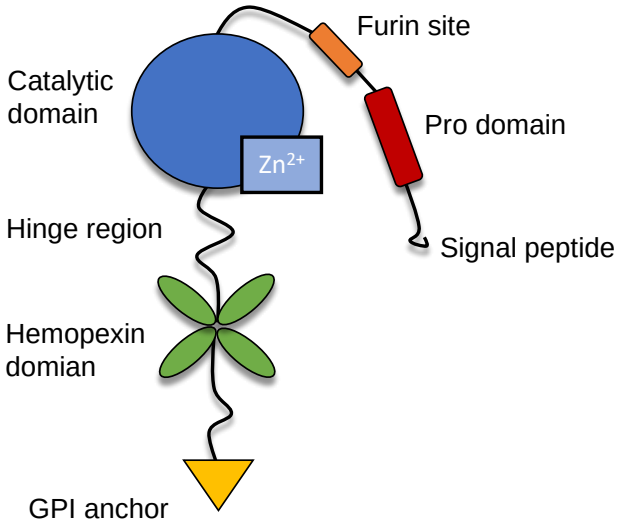

Figure 1-4: Structural domains of MMP17. MMP17 shows structural similarities to the other MMPs by its signal peptide, pro-domain, catalytic domain and hemopexin domain. The presence of the GPI anchor and furin site separates it from most of the other MMPs. (Adapted from (Yip et al., 2019)).

In contrast to other MMPs, MMP17 has a small substrate repertoire among the ECM components and this lack of specificity makes it hard to investigate its functionality (Truong et al., 2016). However, MMP17 shows weak cleaving capacities against fibrinogen, fibrin and gelatin (English et al., 2000; Wang et al., 1999). In addition, some non-ECM substrates have been identified for MMP17; α-2-macroglobulin (English et al., 2000), low density lipoprotein receptor-related protein (Rozanov et al., 2004), proTNF (English et al., 2000), ADAMTS4

(Clements et al., 2011), osteopontin (Martin-Alonso et al., 2015) and alphaM integrin (Clemente et al., 2018).

As with the other MMPs, the previous lack of knowledge around MMP17's biological function was mostly due to the lack of a sensitive system for monitoring and tracking its expression *in vivo*. However, Dr Seiki's group established an *Mmp17*-deficient mouse strain in 2007 (Rikimaru et al., 2007). In this mouse model, illustrated in Figure 1-5, the genomic sequence of *Mmp17* containing the initiation exon and part of the first intron, was replaced with a DNA cassette containing *LacZ* and a nuclear localization signal (NLS). This resulted in a loss of *Mmp17* expression and at the same time the ability to track its expression by active *β-galactosidase* (Rikimaru et al., 2007).

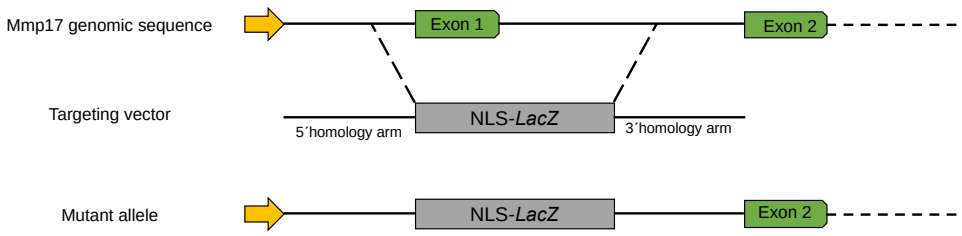

Figure 1-5: Schematic illustration of the *Mmp17*-deficient mouse model. A genomic sequence, containing the initiation exon and part of the first intron, in the *Mmp17* gene was substituted with a *LacZ* cassette encoding the reporter gene *β-galactosidase*. The resulting mutant allele express the *LacZ* cassette under the control of the *Mmp17* promoter (yellow arrow), allowing tracking of *Mmp17* expression. (Adapted from (Rikimaru et al., 2007) (Martin-Alonso, 2016)).

The adult *Mmp17*$^{-/-}$ mice showed normal appearance, behavior, life span and fertility with no major differences detected between the *Mmp17*$^{+/+}$ and M*mp17*$^{-/-}$ strains (Rikimaru et al., 2007). *Mmp17* and *LacZ* mRNA was observed at various levels in several organs and a correlation was found between *Mmp17* expression and *smooth muscle actin* transcripts in the lung, stomach, intestine, testis, ovary and uterus (Rikimaru et al., 2007). Even though *Mmp17* is highly expressed in tissues during several physiological processes, its role in some of these processes has not been described in detail so far. However, it has been suggested to modulate thirst (Srichai et al., 2011), and has been shown to be expressed in murine embryonic development (Blanco et al., 2017). It has also been shown that the lack of MMP17 caused a defect in maturation of vascular SMCs, in addition to altered cell orientation in the tissue and affected ECM connections (Martin-Alonso et al., 2015).

In contrast to the investigation of MMP17 and its physiological function, more research has been done on its function in pathological processes. The function of MMP17 in pathologies is

not only related to its proteolytic function, but also to its non-proteolytic functions (Yip et al., 2019). MMP17 activity has been suggested to be involved in several diseases; breast cancer (Chabottaux et al., 2006), colon cancer (Nimri et al., 2013), head and neck cancer (Huang et al., 2009), osteoarthritis (Clements et al., 2011; Gao et al., 2004; Patwari et al., 2005), thoracic aortic aneurysms and dissections (Martin-Alonso et al., 2015; Papke et al., 2015) and atherosclerosis (Clemente et al., 2018).

The intestine is a highly dynamic structure containing proliferative ISCs, which are highly dependent on appropriate signals and factors from its surroundings during both homeostasis and regeneration after injury. As described, the members of the MMP family play an important role in the regulation of the structural niche in the intestine, by degrading and reorganizing the ECM. SMCs are responsible for producing some of these ECM components, in addition to secreting niche factors. Newer research has suggested a regulatory role of SMCs in the intestinal response and regeneration process after injury. SMCs of the intestine specifically express MMP17, which further have been identified to control SMCs phenotype in vascular tissue. We propose that it is therefore plausible that MMP17 might impact other SMCs, as the intestinal SMCs. Unpublished data from our group shows in fact that the lack of MMP17 does not cause an altered phenotype under homeostatic conditions in the intestine. However, *Mmp17*-deficient mice show impaired regeneration after an acute inflammatory injury caused by DSS treatment. Therefore, we want to further establish the role of MMP17 during the regenerative process in the intestine after injury, with an alternative injury model causing a lower inflammatory response. Finally, determination of MMP17's role in regeneration and response to injury makes this protease of special interest in the future, since it could be a possible therapeutic target in gastrointestinal diseases and cancers.

2 Objective

MMP17 shows distinct features compared to other members in its family, indicating unique functions and possible implications in different pathologies. In the intestine, MMP17 has been demonstrated to be specifically expressed in SMCs of the muscularis mucosae and muscularis externa, with unknown functions and substrates. Unpublished data from our group indicates that lack of MMP17 leads to impaired regeneration in mice after an acute inflammatory injury induced by a DSS treatment. We therefore wanted to further investigate if MMP17 could impact the regeneration response using a different injury model, such as radiation exposure, which causes a lower inflammatory response.

The main objective purposed for this study is:

- Determine if MMP17 plays a role in the regenerative response to the intestinal injury produced by radiation exposure.

3 Methodology

3.1 Mouse model

The *Mmp17*$^{-/-}$ mouse model has been described previously (see section 1.4.1 and Figure 1-5) (Rikimaru et al., 2007). All mice were kept in sterile conditions in accordance to guidelines set by the Comparative Medicine Core facility at NTNU. All experiments preformed on mice were ethically approved and evaluated by the Norwegian Food and Safety Authorities (FOTS).

3.2 Irradiation of mice

Mmp17$^{+/+}$ and *Mmp17*$^{-/-}$ mice were anesthetized using Ket/Xyl (ketamine 50 mg/ml, xylazine 20 mg/ml in water, mixed 1:0,25:3,75 (volume)). Mice were irradiated with photon-radiation with an energy of 6MV from a Versa HD Linear Accelerator (Elektra Instrument AB, Stockholm, Sweden).

The mice were placed in a perspex box on top of a radiation table, composed of 1 cm plate of solid water. The table was adjusted so that the horizontal isocenter plane (100 cm from the source) was centered on the mice. They were irradiated from underneath with a radiation field of 35 x 35 cm in the isocenter plane. The mice were exposed to 10 Gy of whole-body radiation in one fraction. Mice were monitored for optimal recovery (antisedan was injected) after irradiation.

Mice were euthanized 1 day, 3 days or 6 days after irradiation, in addition to un-irradiated mice. The mice were weighed before irradiation and daily until euthanized. After euthanization, the small intestine and the colon were harvested, and the length was measured.

3.3 Tissue fixation and processing

Living tissues from an organism will quickly alter after harvesting, so fixation is a way to preserve the tissues in a life-like condition for further analysis and research. This is normally achieved through immersing the tissue in a fixative solution, often using formaldehyde, that acts as an enzyme blocker (Cook & Warren, 2015; Kim et al., 2016). When formaldehyde polymerizes it forms paraformaldehyde (PFA) and this is often used instead of formaldehyde since it is more reliable and purer (Cook & Warren, 2015).

After fixation, the tissue needs extra support, which is achieved through embedding in paraffin wax. Paraffin wax is molten at 60°C, but it is solid at room temperature. However, tissues cannot simply be embedded in paraffin in one single step, since the tissue contains water, which is immiscible with wax (Cook & Warren, 2015). The water in the tissue is replaced with wax in several intermediate steps and this is called processing. This happens in two stages; first dehydration, which removes the water, and clearing, which replaces the dehydrating agent with a reagent that is miscible with wax. The tissues are then impregnated with wax, placed in a mold and the wax is solidified. (Cook & Warren, 2015)

3.3.1 Experimental procedure

After measuring the length, the small intestine was approximately separated into the duodenum, jejunum and ileum. The distinct parts of the small intestine and the colon were cleaned with phosphate-buffered saline (PBS) and rolled into swiss rolls. This was done by cutting the tissues longitudinally and rolling them with the luminal side facing up, onto wooden sticks (Moolenbeek & Ruitenberg, 1981). The tissues were then fixated with 4% PFA overnight and processed automatically by a Lecia ASP300S tissue processor the following day. After processing, the tissues were embedded in paraffin, cut into 4 μm thick sections using a microtome and attached to glass slides.

3.4 Hematoxylin and eosin staining

Hematoxylin and eosin (H&E) staining is one of the principal stainings in histology. Hematoxylin is not a dye in itself and needs to be oxidized to hematein combined with a mordant (usually aluminum salts) (Cook & Warren, 2015; Fischer et al., 2008). This creates a basic and positively charged solution that stains acidic and negative structures, mostly DNA and RNA, that will turn the nucleus of the cell violet/blue. Eosin is often used to counterstain with hematoxylin and is a variety of related acidic and negative dyes. It will stain basic and positive structures in various shades of pink and red, and these include most of the structures in the cytoplasm and connective tissue (Cook & Warren, 2015; Fischer et al., 2008). Before any staining can occur, the paraffin wax needs to be removed tissue and the tissue needs to be rehydrated. This is because of the aqueous solutions used in the staining techniques, which is immiscible with wax (Cook & Warren, 2015).

3.4.1 Experimental procedure

Before staining the paraffin wax must be removed and the tissue rehydrated. The tissue sections were heated in an oven at 60°C for 20-30 minutes, prior to being placed in neo-clear (a less toxic version of xylene) for 2 x 5 minutes. Then the sections were rehydrated utilizing a transfer through graded alcohols (100%, 96% and 70%) for approximately 1 minute each, before finally being placed in water. The tissue sections were then stained with hematoxylin for approximately 30 seconds and washed in warm water. The sections were then stained with eosin for approximately 3 minutes and washed in warm water. The glass sections were rehydrated through a series of alcohols (80%, 96% and 100%) and placed in neo-clear. The slides were then mounted using aqueous mounting medium and coverslips were added.

After H&E staining, the tissue sections were imaged and further analyzed (see section 3.7).

3.5 Immunofluorescence

Immunofluorescence (IF) is a staining technique were antibodies are used to detect and localize target proteins (antigens), using the principle that antibodies bind specifically to antigens in biological tissues. In IF the antibody is tagged with a fluorochrome and can be visualized with a fluorescent microscope (Cook & Warren, 2015). The labelling of a target protein can be done by a direct technique, using only a fluorochrome-conjugated primary antibody, or by an indirect technique, using a primary antibody and a secondary antibody that is specific to the primary antibody. The indirect way has the advantage that it amplifies the signal, which is important if the target protein is not highly expressed in the tissue. (Cook & Warren, 2015)

Before staining can occur, restoring full immunoreactivity of the sections is required, as fixation and processing often can alter the antigens. The unmasking of the antigen occurs through a technique called antigen retrieval and is usually performed either through the use of enzymes or heat (Chen et al., 2010). In heat retrieval the sections are usually in an antigen retrieval solution and heated with a microwave. The power and time of the heating depends on the antigens to be unmasked and the fixation of the tissue (Chen et al., 2010; Cook & Warren, 2015).

Before incubation with primary antibodies, all potential nonspecific binding sites in the tissue section needs to be blocked, to prevent nonspecific antibody binding. Blocking solutions often

contain natural host serum, because it carries antibodies that bind to reactive sites and prevent nonspecific binding of the secondary antibodies used in the assay (Cook & Warren, 2015). The critical factor is to use serum from the source species of the secondary antibody. Besides host serum, blocking solutions often contain bovine serum albumin (BSA), which also binds to nonspecific sites in the tissue sample (Chen et al., 2010). Lastly, reagents that allow permeabilization are often added to the solution. This allows intracellular structures to become accessible to the antibodies used. Classical detergents like Triton X-100 and NP-40 are often used, in addition to Tween 20, saponin and digitonin (Chen et al., 2010; Cook & Warren, 2015). Furthermore, the primary- and secondary antibodies are diluted in a buffer before application, which often contains some of the same components as the blocking solution. This aids the stability of the antibody, proper diffusion into the tissue and prevents further nonspecific binding (Kim et al., 2016).

3.5.1 Experimental procedure

The tissues were deparaffinized by heating them in an oven at 60°C for 20-30 minutes and transferred into neo-clear twice for 5 minutes each. Then the slides were rehydrated by moving them through dishes containing gradually decreasing concentrations of ethanol (100%, 95% and 70%) and placed in water for 3 minutes. For antigen retrieval, the slides were covered in citrate buffer pH 6 and placed in a microwave. The tissue slides were heated at 800W until the buffer was boiling, and then at 90W for 15 min. The slides were then cooled in the buffer for 20 minutes.

Tissue slides were then washed in water for 1-2 minutes and dried off. The sections were marked with a hydrophobic pen, to ensure that they did not dry out during the incubation period. A blocking buffer containing 2% normal goat serum (NGS), 1% BSA, 0.2% Triton X-100 and 0.05% Tween 20 in 1X PBS was added to each tissue section and incubated in a humid chamber under a lid for 1 hour. The blocking buffer was also used as a dilutant for both primary- and secondary antibody solutions. The blocking buffer was removed after 1 hour and a primary antibody solution was added; Ki67 (ThermoFisher Scientific, #62249) in a 1:250 dilution. The slides incubated over-night in a staining box with a lid at 4°C.

The next day the tissue slides were washed 3 times with Tris-buffered saline and Tween (TBST) for 5 minutes. The secondary antibodies, Goat anti-Rabbit IgG Alexa Fluor 488 (Invitrogen, #A-11034) in a 1:500 dilution, Ulex Europaeus Agglutinin 1 (UEA-1) (Vector Laboratories,

#RL1062) in a 1:500 dilution and Hoechst (ThermoFisher Scientific, #62249) in a 1:5000 dilution, were added to the slides and incubated for 1 hour in room temperature. The slides were then washed 3 times with TBST for 5 minutes and then in water 2 times for 2-3 minutes each. The slides were mounted with Fluoromount-G™ (Invitrogen, #00-4958-02) and coverslips were added. The slides were stored in a staining box in a cold room (4 °C).

The immunofluorescent staining using Cleaved Caspase-3 (CAS3) was performed using the same protocol as with the Ki67 staining, but there were a few alterations to optimize the staining. Antigen retrieval was performed in EDTA buffer with a pH of 9. Slides were then cooled in the buffer for 2 hours after the antigen retrieval. The components in the blocking buffer had different concentrations; 5% NGS, 5% BSA, 0.3% Tx-100 and 0.05% Tween 20. The primary antibodies used were Cleaved Caspase-3 (Cell Signaling Technology, #9661S) in a 1:200 dilution and β-catenin (Santa Cruz, #130917) in a 1:200 dilution. In addition, the slides were incubated with the secondary antibodies; Goat anti-Rabbit IgG Alexa Fluor 488 (Invitrogen, #A-11034) in a 1:500 dilution, Goat anti-Mouse IgG Alexa Fluor 647 (Invitrogen, #A-21236) in a 1:500 dilution, UEA-1 (Vector Laboratories, #RL1062) in a 1:500 dilution and Hoecst (ThermoFisher Scientific, #62249) in a 1:5000 dilution, for 2 hours.

After Ki67 and CAS3 IF staining, the tissue slides were imaged (see section 3.7).

3.6 In situ hybridization

In situ hybridization (ISH) is a detection method that uses labelled probes to identify and localize specific strands of DNA or RNA in a tissue section. The probes are complementary strands to the target DNA or RNA and can be labelled in several different ways (Cook & Warren, 2015; Nouri-Aria, 2008). The methodology for ISH is quite variable, since this needs to be optimized for the particular probes and tissues used. However, there are some general steps. First, if the tissue is embedded in wax, this needs to be removed and the tissue needs to be rehydrated. Then the tissue is normally digested with a proteinase (to help free DNA or RNA from its binding to proteins) (Cook & Warren, 2015). If the target sequence is DNA, this needs to be separated before adding the probe, and later annealed back together (Cook & Warren, 2015). Then the tissue is incubated with probe(s), where it will hybridize to its target sequence. There can be several amplification steps following this hybridization, to strengthen the signal of the probe. Lastly, the tissue is dehydrated and mounted (Cook & Warren, 2015).

3.6.1 Experimental procedure

The ISH was performed using RNAscope 2.5 HD Detection Reagents-BROWN (ACD Bio, #322310), RNAscope H202 & Protease Plus reagents (ACD Bio, #322330) and the probe against *Olfactomedin-4* (*Olfm4*) (ACD Bio, #311831). The ISH was preformed according to the manufactures protocol.

After ISH the tissues were imaged and further analyzed (see section 3.7).

3.7 Microscopy and image analysis

Light microscopes use a system of lenses and visible light to magnify small objects (Thorn, 2016). Together, a lighting system and a condenser lens focuses the light onto the specimen, which is picked up by the above objective lens. This light is then focused on the focal plane of the objective lens and this together with the ocular lens (eyepiece) creates a magnified image of the specimen (Cook & Warren, 2015; Lodish et al., 2000).

Fluorescence microscopes are often used in histology to image sections that are stained with fluorescent probes (Cook & Warren, 2015). This type microscope consists of two filters, one below the specimen and one above the specimen. The filter below absorbs all of the long-wavelengths, so the specimen is illuminated only by short wavelengths. The second filter blocks out this short-wavelength light, leaving a black background (Cook & Warren, 2015; Thorn, 2016). Confocal is a form of fluorescence microscope which uses a very small aperture (pinhole) at the back of the focal plane of the objective to restrict flare from out-of-focus light. This produces a very thin depth of field but requires the specimen to be scanned with illuminating light, rather than the whole of the specimen being illuminated. This usually involves a laser in combination with a dichroic mirror (Cook & Warren, 2015; Thorn, 2016). The image is created by reconstruction of the specimen using digital technology. If the specimen is thick, it is possible to give series of aligned optical slices through the whole sections, making a three-dimensional structure and which is called a Z-stack (Cook & Warren, 2015).

3.7.1 Experimental procedure

Images from the H&E staining and ISH were obtained using EVOS FL Auto 2 Cell Imaging System (Thermo Fisher, Norway) with an EVOS^{TM} 10x Objective (Achromat) or an Olympus

20x Objective (Super-Apochromat). The length of the crypts and villi were measured using the image analysis software Fiji (Schindelin et al., 2012). The blind injury score was assessed using the following criteria; the length of the crypts and villi, loss of crypts and villi, presence of immune infiltrate and villus blunting. The score was performed by a researcher blind for the sample genotype. The positive staining in ISH *Olfm4* was quantified using Fiji (Schindelin et al., 2012).

Images from Ki67 and CAS3 stainings were obtained from Zeiss LSM 5 Live and Zeiss 880 Airyscan Fast using a Zeiss 20x objective (Plan-Apochromat 20x/0.8). The images were captured using Z-stack and presented as maximal projections.

3.8 Statistical analysis

To check for significance a one-way or two-way ANOVA followed by Bonferroni's multiple comparisons test, a Mann-Whitney test or an unpaired t-test was performed using GraphPad Prism 5.00 (GraphPad Software, La Jolla California, USA). The statistical analyses performed in each experiment are explained in detail in the corresponding figure legend. Data are presented as mean ± standard error of the mean (SEM) and the differences were considered statistically significant at $p < 0.05$; *p-value < 0.05, **p-value < 0.01 and ***p-value < 0.001.

4 Results

4.1 Irradiation set up and phenotypical evaluation shows efficient intestinal damage

The mouse intestinal epithelium is capable of regenerating when it is exposed to radiation doses below 14 Gy (Metcalfe et al., 2014). It was decided to collect tissues 1, 3 and 6 days after irradiation of *Mmp17*$^{+/+}$ and *Mmp17*$^{-/-}$ mice. Day 1 was used as a control for equal damage between the two genotypes, while tissues from day 3 and day 6 were picked to study the regeneration process back to homeostatic conditions. Un-irradiated tissues from *Mmp17*$^{+/+}$ and *Mmp17*$^{-/-}$ were also included as a control for undamaged tissue. Doses over 14 Gy can cause an acute radiation syndrome, where loss of body weight is a common clinical manifestation of the progressive form. Even though the mice in this study only received a dose of 10 Gy, body weight is a good indication of the overall effect of the radiation. 1 day post-irradiation both *Mmp17*$^{+/+}$ and *Mmp17*$^{-/-}$ mice showed a 5% loss of body weight (Figure 4-1 A). We presume that this is due to the anesthetics, which have been reported to cause a loss of body weight in rodents (Blaha & Leon, 2008; Dholakia et al., 2017; Welberg et al., 2006). 6 days after radiation exposure both *Mmp17*$^{+/+}$ and *Mmp17*$^{-/-}$ showed a loss of weight between 10-15%, but there was no difference between the two genotypes at any time points evaluated after irradiation. The effect of irradiation was also assessed by measuring the length of the small intestine and the colon, since shrinkage of the intestine is a common feature after injury. There was no difference between the length of the small intestine or the colon between *Mmp17*$^{+/+}$ and *Mmp17*$^{-/-}$ mice at the various time points (Figure 4-1 B and Figure 4-1 C). These results demonstrate that both mouse strains had similar responses to the radiation exposure in the terms of body weight and length of intestine.

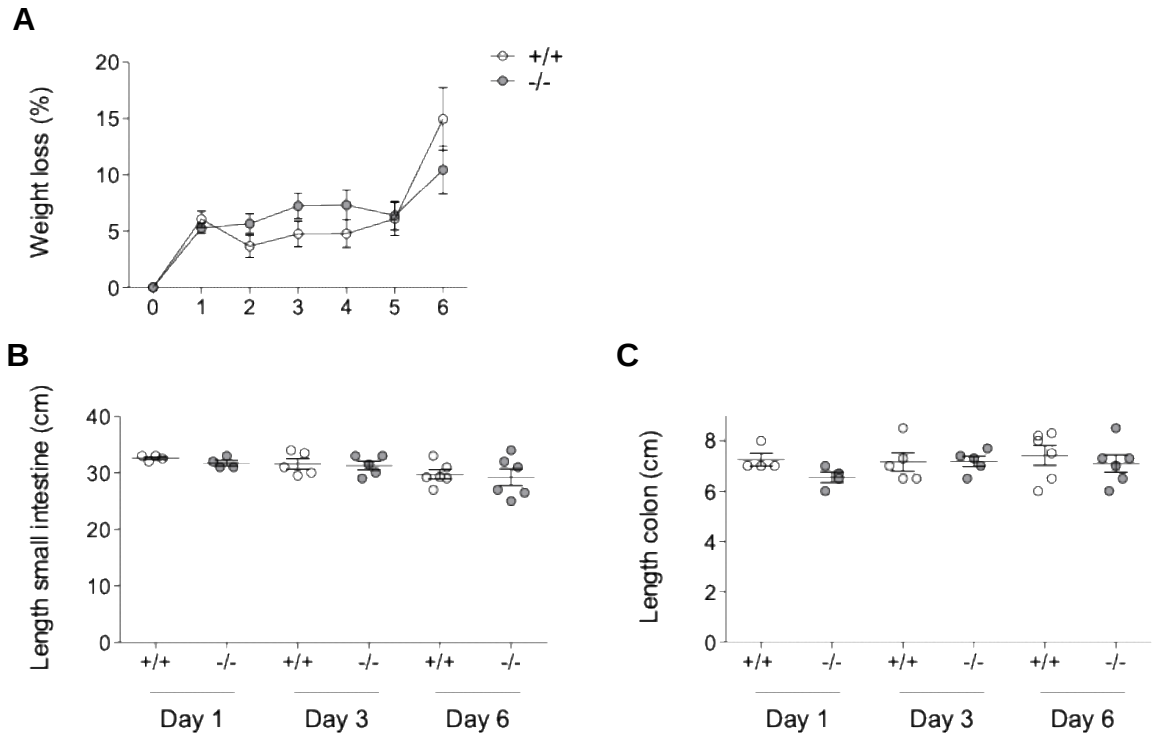

Figure 4-1: No difference in weight or length of intestine between *Mmp17*$^{+/+}$ and *Mmp17*$^{-/-}$ after irradiation. (**A**) % of weight loss in *Mmp17*$^{+/+}$ and *Mmp17*$^{-/-}$ mice after irradiation from 0 to 6 days.. (**B**) Length of small intestine between *Mmp17*$^{+/+}$ and *Mmp17*$^{-/-}$ mice 1, 3 or 6 days after irradiation. (**C**) Length of the colon *Mmp17*$^{+/+}$ and *Mmp17*$^{-/-}$ mice 1, 3 or 6 days after irradiation. For (**A-C**) at least a n = 4 per genotype were analyzed per time point. Error bars in (**A-C**) present mean ± SEM and data were analyzed in **(A)** by two-way ANOVA followed by Bonferroni's posttest and **(B-C)** by one-way ANOVA followed by Bonferroni's multiple comparison test.

To validate if the irradiation was effective, we analyzed apoptosis of stem cells in both the small intestine and the colon. An IF staining with CAS3 was performed in control and day 1 sections of small intestine (ileum) and colon. Throughout all experiments, it was decided to focus on the ileum from the small intestine and this because it is closer in both structure and proximity to the colon. This would make the comparison with the previous DSS experiment easier, as the colon was the tissue effected by the DSS administration. CAS3 specifically marks cells that are going through apoptosis. The un-irradiated control tissues contained no positive cells at the bottom of the crypt in either ileum or colon, indicative of no apoptosis during homeostasis (Figure 4-2). At day 1 both tissues contained CAS3 positive cells at the bottom of the crypts and there was no difference between *Mmp17*$^{+/+}$ and *Mmp17*$^{-/-}$ mice (Figure 4-2). This demonstrates that irradiation induces cell death in actively cycling ISC at the same levels in both tissues and genotypes. In addition, it is normal to observe positive CAS3 cells at the top of the villus in the small intestine or at the top of the epithelium in the colon at any time point.

This is due to the fact that the epithelial cells go through anoikis and are shed into the intestinal lumen.

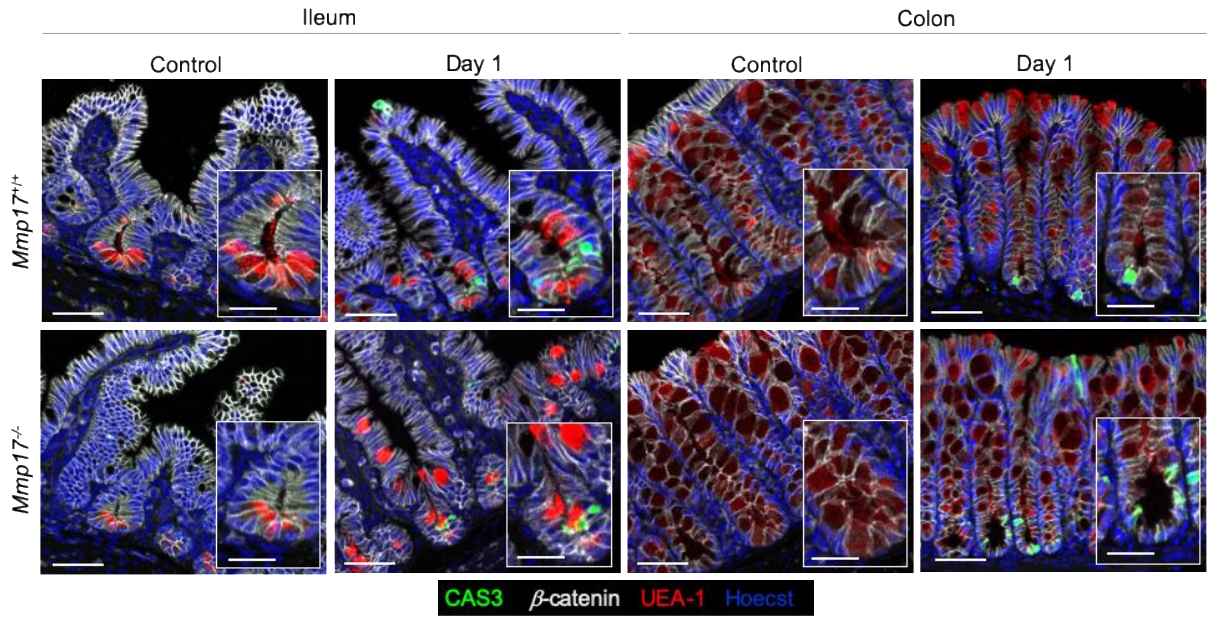

Figure 4-2: Irradiation caused cellular apoptosis at the bottom of crypts in both small ileum and colon at 1 day post-irradiation. Representative confocal microscopy images of Cleaved Caspase-3 (CAS3) stained sections from *Mmp17*$^{+/+}$ and *Mmp17*$^{-/-}$ in both ileum and colon, control and 1 day post-irradiation. The nuclei are stained blue (Hoechst) and glycoproteins and glycolipids in red (UEA-1). Images are representative of at least a n = 3 per genotype at every time point. The scale bar indicates 50 μm and 25 μm in insets.

4.2 Intestinal injury is sustained in ileum in *Mmp17*$^{-/-}$ mice after irradiation

After exposure to radiation the epithelium in the intestine goes through structural changes. First because of the damage caused by the loss of ISCs and then later to heal the damage (Withers et al., 1970; Withers & Elkind, 1970). To determine the changes in tissue architecture after radiation exposure in the ileum, H&E stainings of ileum sections were performed. There was a clear reduction in the size of both crypts and villi at day 1 in the ileum, but there was no obvious difference between *Mmp17*$^{+/+}$ and *Mmp17*$^{-/-}$ mice (Figure 4-3). This indicates that both genotypes display the same level of injury after irradiation. However, during the regeneration phase, at day 3, the crypt length was expected to be enlarged due to the increased proliferation of the surviving cells. This structural feature was present in the H&E stainings, but the *Mmp17*$^{-/-}$ mice appeared to have even longer crypts than the *Mmp17*$^{+/+}$ mice (Figure 4-3). In addition, we observed more crypt loss and villus blunting in the *Mmp17*$^{-/-}$ genotype. These observations are similar 6 days after irradiation, where the *Mmp17*$^{-/-}$ had noticeable longer crypts and shorter and wider villi (Figure 4-3). The observations made in the H&E stainings were further

confirmed by a blind injury score, which were performed by a second researcher. This method was based on assigning the tissues a score between 0-2, dependent on level of damage. The criteria evaluated in this score model were: the level of inflammatory cell infiltrates and changes in the epithelium, including increased crypt and villus length, crypt and villus loss and villus blunting. The chosen criteria for this score was based on previously reported features after irradiation (Metcalfe et al., 2014) and also scoring standards after damage in inflammatory mice models (Erben et al., 2014). Both genotypes had a low injury score 1 day after radiation, while they both got higher scores 3 days after (Figure 4-4 A and B). 3 days post-irradiation, the *Mmp17*$^{-/-}$ mice got a statistically significant higher score compared to the *Mmp17*$^{+/+}$ mice. The difference in the injury level was still present 6 days post-irradiation, where *Mmp17*$^{-/-}$ mice showed a high injury score, while *Mmp17*$^{+/+}$ were close to 0, indicative of mucosal healing (Figure 4-4 C).

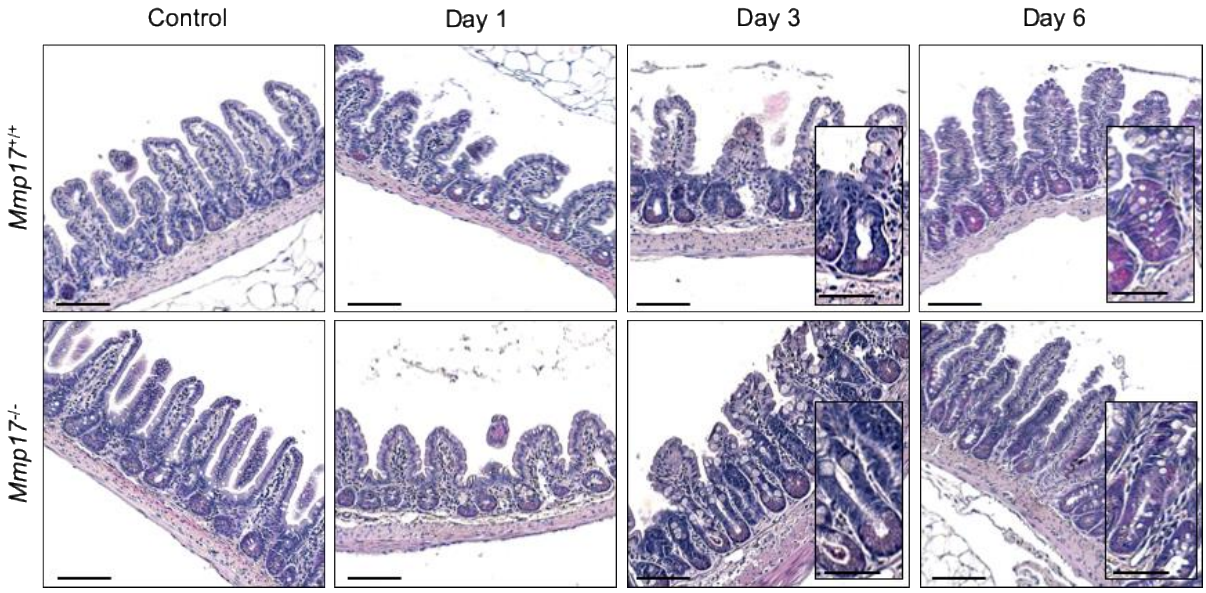

Figure 4-3: *Mmp17*$^{-/-}$ ileum shows more changes in mucosal architecture and no repair compared to *Mmp17*$^{+/+}$. (**A**) Representative H&E stained sections from *Mmp17*$^{+/+}$ and *Mmp17*$^{-/-}$ ileum, control and 1, 3, and 6 days post-irradiation. Images are representative of at least a n = 3 per genotype per time point. The scale bar indicates 100 μm and 50 μm in insets.

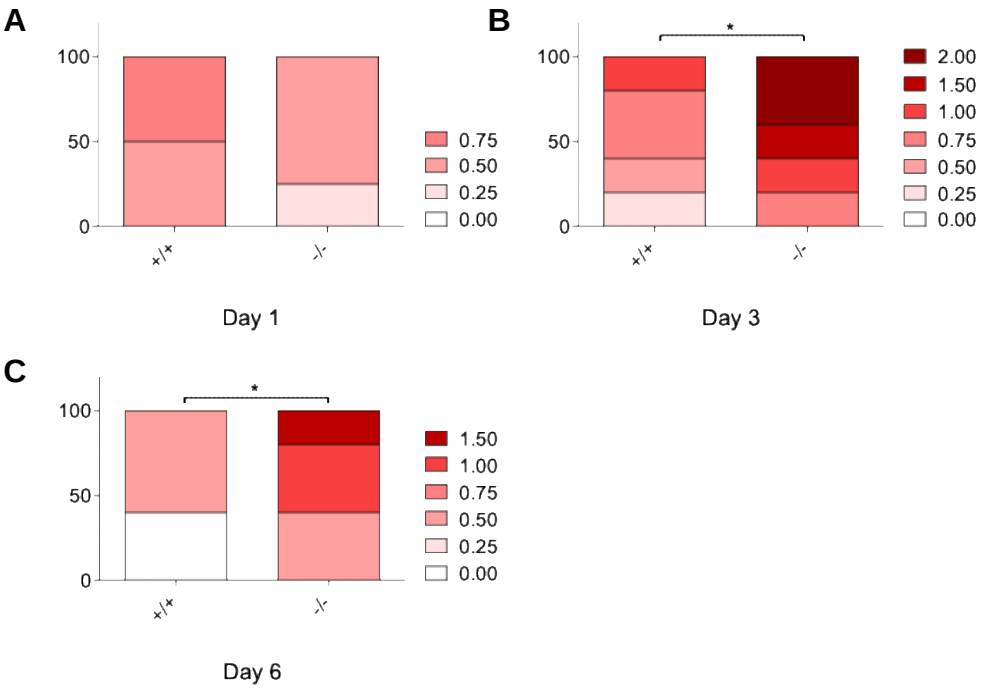

Figure 4-4: *Mmp17*$^{-/-}$ shows sustained damage after irradiation. (**A-C**) Blind injury score in *Mmp17*$^{+/+}$ and *Mmp17*$^{-/-}$ ileum 1, 3 and 6 days post-irradiation, presented as the total percentage of mice within a given score. At least a n = 4 was scored per genotype per time point. Data were analyzed by a non-parametric Mann-Whitney test (p* < 0.05).

To check some the parameters assessed by the blind injury score, the length of crypts and villi were measured. The lengths of villi and crypts showed a decrease 1 day after irradiation, with equal levels in both genotypes, indicating the occurrence of a similar injury level (Figure 4-5 A and B). 3 days-post radiation exposure, the *Mmp17*$^{-/-}$ mice had noteworthy longer crypts and shorter villi than the *Mmp17*$^{+/+}$ mice, confirming the sustained damage in the *Mmp17*$^{-/-}$ at this timepoint (Figure 4-5 C). Crypts and villi length were not significantly different at day 6, but there was still a trend of shorter villi in the *Mmp17*$^{-/-}$ mice. Since blunted villi were observed at a higher frequency in the *Mmp17*$^{-/-}$ mice in the H&E staining at day 3, we also measured the width of the villi at this timepoint. There was a trend that *Mmp17*$^{-/-}$ overall had wider villi than the mice expressing *Mmp17*, but it was not significant. Together, the H&E stainings, the blind injury score and the measurements of crypt and villus length indicate that mice lacking the expression of *Mmp17* have impaired regeneration compared to mice expressing *Mmp17* after irradiation.

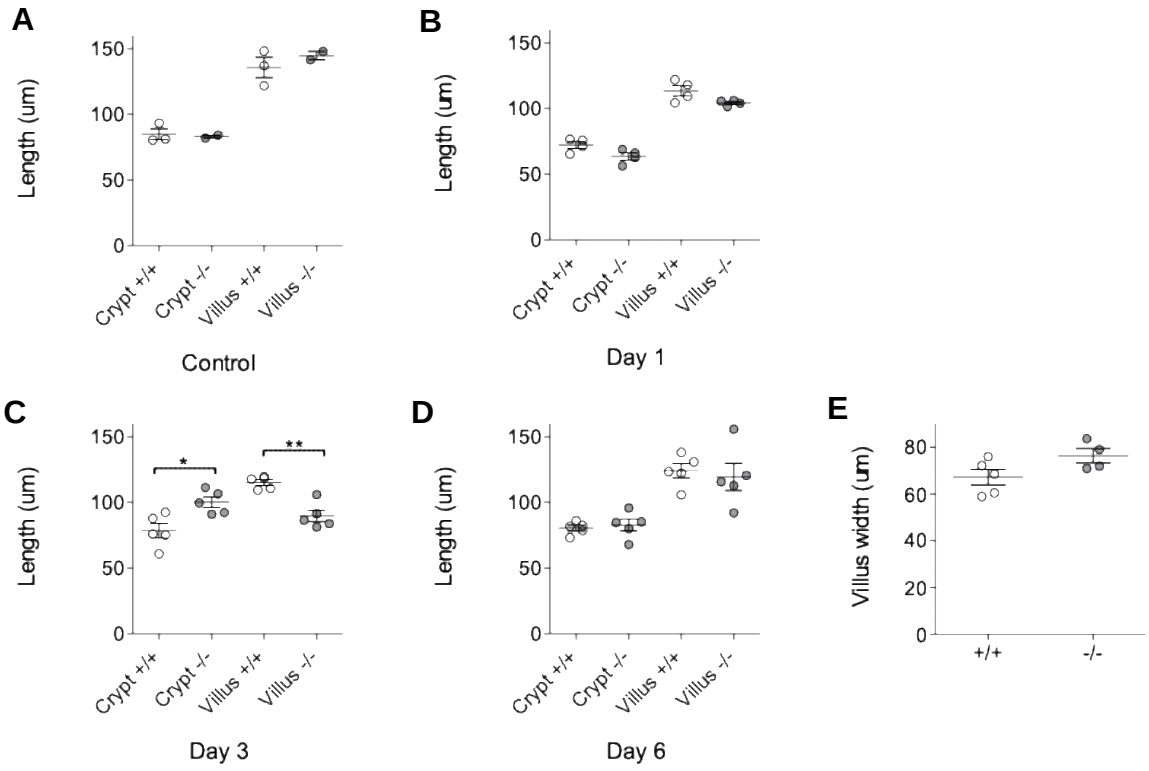

Figure 4-5: Elongated crypts and shorted villi indicative of sustained damage in *Mmp17*$^{-/-}$ irradiated ileum. (**A-E**) Average crypt and villus length in *Mmp17*$^{+/+}$ and *Mmp17*$^{-/-}$ ileum control and 1, 3 and 6 days after irradiation. At least n = 4 were measured per genotype per time point and approximately 20-30 crypts and villi were measured per mouse. (**E**) Average villus width in *Mmp17*$^{+/+}$ and *Mmp17*$^{-/-}$ ileum 3 days post-irradiation. At least n = 4 were measured per genotype per time point and approximately 20-30 villi were measured per mouse. Error bars in (**A-E**) present mean ± SEM and data in **(A-D)** were analyzed with one-way ANOVA followed by Bonferroni's multiple comparisons test ($p^* < 0.05$, $p^{**} < 0.01$) and in **(E)** by a non-parametric Mann-Whitney test.

Irradiation induced ISC apoptosis 24 hours after injury (Figure 2-2) in both colon and small intestine. As with the ileum, structural alterations were addressed through performing a H&E staining on tissue sections from the colon. 1 day after radiation exposure the crypts seemed to be shorter in size in the colon in both *Mmp17*$^{+/+}$ and *Mmp17*$^{-/-}$ mice (Figure 4-6). In addition, it was identified a presence of edema in the submucosa 1 and 3 days after irradiation in colon tissues. Edema is characterized by accumulation of fluid and is associated with damage, occurring in diseases like IBD (Moore-Olufemi et al., 2009; Young et al., 2014). Besides this, the colon showed no extensive signs of damage and no difference in tissue structure were identified between *Mmp17*$^{-/-}$ and *Mmp17*$^{+/+}$ mice. As with the ileum, a blind injury score was performed to verify the observations from the H&E staining. The injury score was carried out the same way as previously mentioned, following the same criteria. The score in both *Mmp17*$^{+/+}$ and *Mmp17*$^{-/-}$ was low at both at 1 day, 3 days and 6 days after irradiation, and there was no difference between the two genotypes (Figure 4-7).

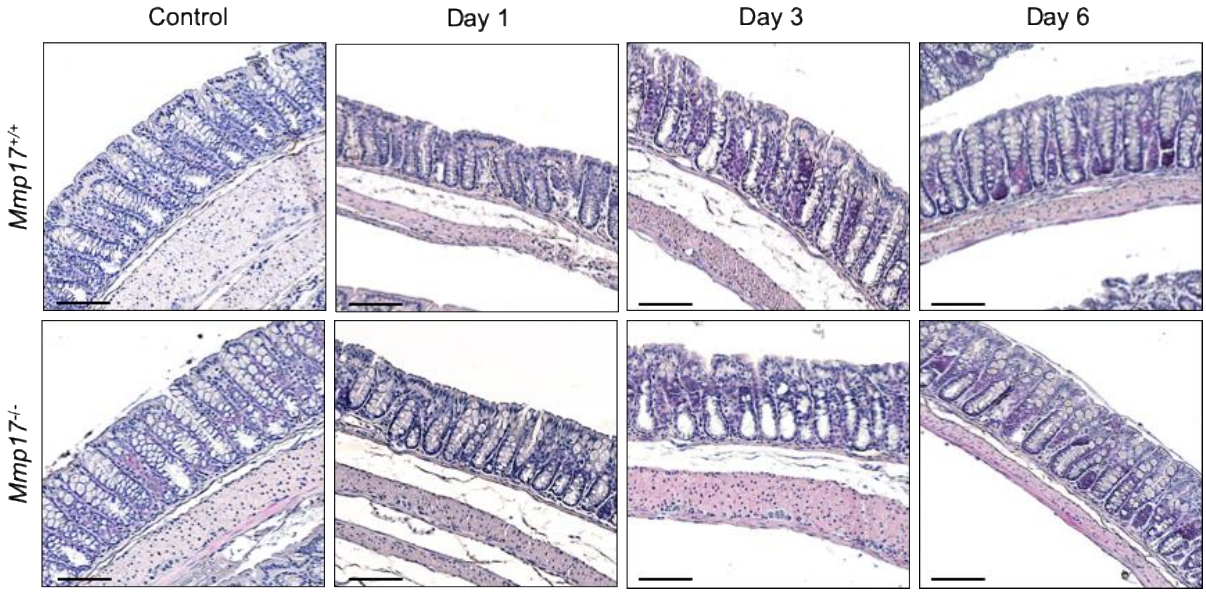

Figure 4-6: No structural significant differences in colon after irradiation. Representative H&E stained sections from *Mmp17*$^{+/+}$ and *Mmp17*$^{-/-}$ colon, control and 1, 3, and 6 days post-irradiation. Images are representative of at least a n = 4 per genotype per time point. The scale bar indicates 100 μm.

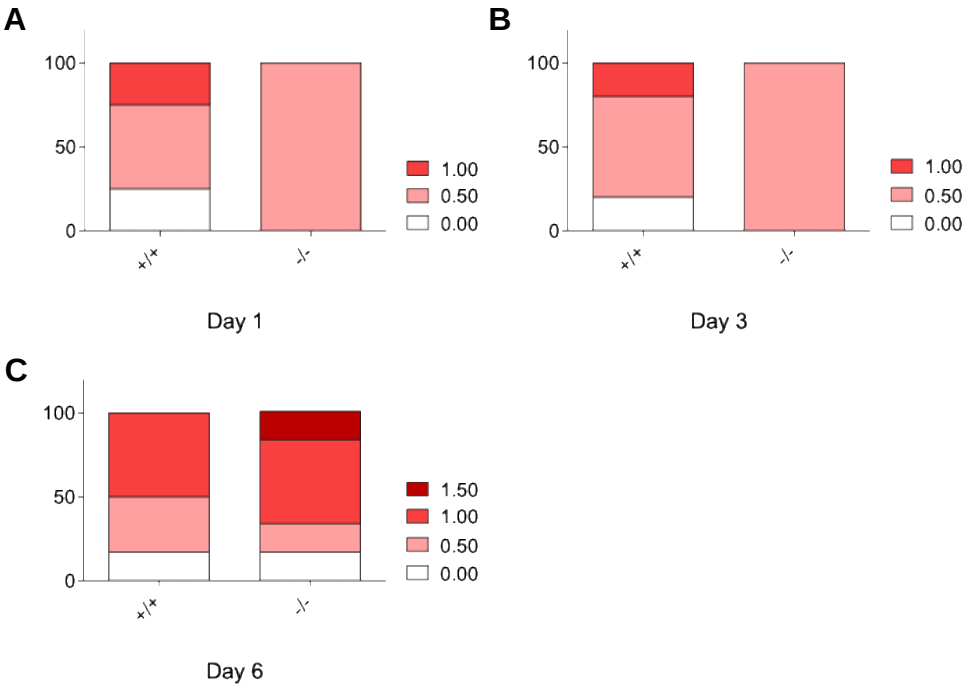

Figure 4-7: No difference in level of damage and repair in irradiated colon. (**A-C**) Blind injury score in *Mmp17*$^{+/+}$ and *Mmp17*$^{-/-}$ colon 1, 3 and 6 days post-irradiation. At least a n = 4 was scored per genotype per time point. Data were analyzed by a non-parametric Mann-Whitney test.

To check some of the parameters assessed by the blind injury score, the length of crypts was measured in the colon. 1 day post-radiation exposure the crypts showed a decreased length compared to the ones in the control sections (Figure 4-8 A and B). This confirms the observation made in the H&E staining. Apart from this, there were no changes in the length or differences between the crypts in *Mmp17*$^{+/+}$ and *Mmp17*$^{-/-}$ mice (Figure 4-8 C and D). Collectively, these data demonstrate that the colon does not display any drastic signs of damage after radiation exposure, except for a small decrease in crypt length and the presence of edema.

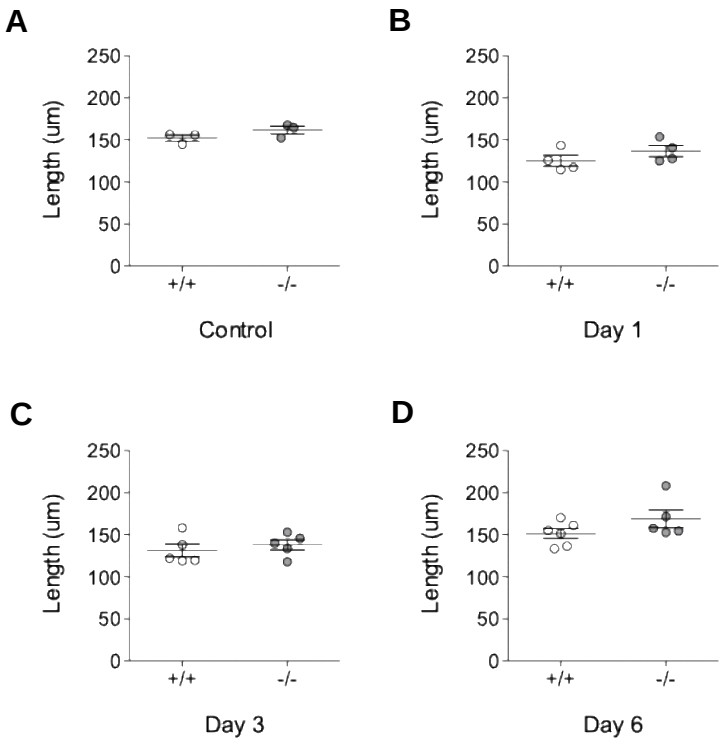

Figure 4-8: Colon crypt length is not different after irradiation in *Mmp17*$^{+/+}$ and *Mmp17*$^{-/-}$ mice. (**A**-**D**) Average crypt length in *Mmp17*$^{+/+}$ and *Mmp17*$^{-/-}$ colon, control and 1, 3 and 6 days after irradiation. At least n = 4 were measured per genotype per time point and approximately 30-50 crypts were measured per mouse, from both the distal part and proximal part of the colon. Data were analyzed by a non-parametric Mann-Whitney test.

4.3 Confirmation study in small intestine shows impaired regeneration

To verify and provide evidence of reproducibility of previous results, irradiation of *Mmp17*$^{+/+}$ and *Mmp17*$^{-/-}$ mice were repeated. The mice were euthanized 3 days after exposure and the ileum was harvested, since the previous results were most significant at this time point and in this tissue. A H&E staining and blind injury score was performed (Figure 4-9 A and B). We observed a trend to more damage in the *Mmp17*$^{-/-}$ 3 days after irradiation, even though not statistically significant (Figure 4-8 A). It was observed a presence of significantly shorter and

thicker villi in the *Mmp17*$^{-/-}$ mice (Figure 4-8 B and C), which points to a higher number of blunted villi, indicative of increased damage in *Mmp17*$^{-/-}$ mice 3 days post radiation.

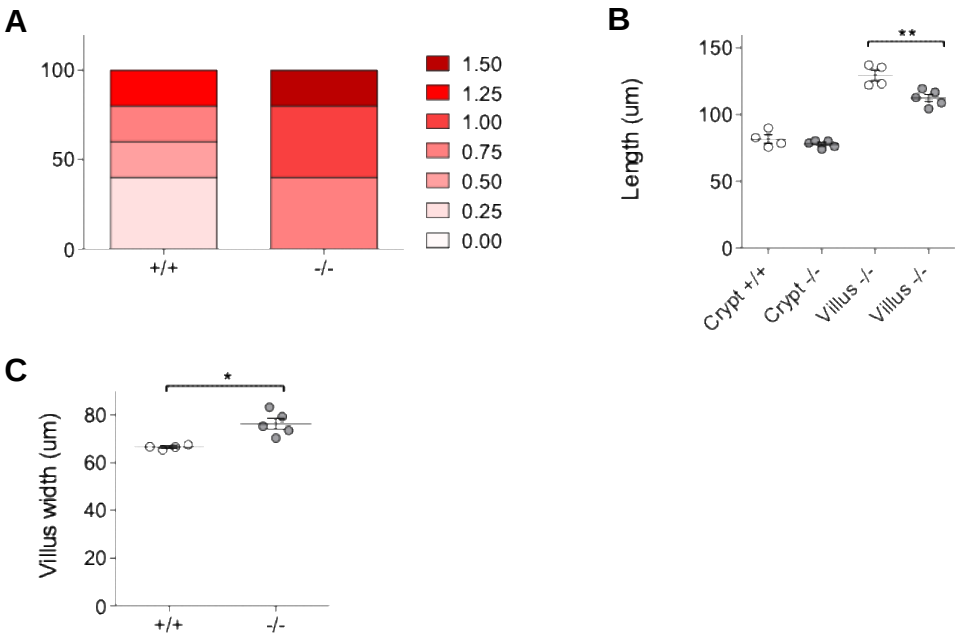

Figure 4-9: Repetition of irradiation shows same increased features of injury in *Mmp17*$^{-/-}$ mice. (**A**) Blind injury score in *Mmp17*$^{+/+}$ and *Mmp17*$^{-/-}$ ileum 3 days post-irradiation. (**B**) Average crypt and villus length in *Mmp17*$^{+/+}$ and *Mmp17*$^{-/-}$ ileum 3 days post-irradiation. Approximately 20-30 crypts and villi were measured per mouse. (**C**) Average villus width in *Mmp17*$^{+/+}$ and *Mmp17*$^{-/-}$ ileum 3 days post-irradiation. Approximately 20-30 villi were measured per mouse. In (**A-**C) a n = 4 were analyzed per genotype per time point. Data were analyzed in (**A**) by non-parametric Mann-Whitney ($p>0.05$), in **(B)** by one-way ANOVA followed by a Bonferroni's multiple comparisons test ($p^{**} < 0.01$) and in **(C)** by a non-parametric Mann-Whitney test ($p^{*} < 0.05$). Error bars in **(B-C)** mean ± SEM.

A combination of the two performed experiments were conducted in order to increase the sample size, so it would more reliably reflect the population. The data from both irradiation procedures were combined for statistical analysis at day 3. Even though the injury score in the second irradiation experiment did not prove to be statistically different, joining the two experiments showed that mice lacking MMP17 had a statistically significant higher injury score than the *Mmp17*$^{+/+}$ mice (Figure 4-10 A). The length of the crypts was not obviously different when joining the two radiation experiments, but the villi was still significantly shorter in the *Mmp17*$^{-/-}$ mice (Figure 4-10 B). This was also demonstrated by the two radiation experiments on their own. The combined villus width demonstrated that the *Mmp17*$^{-/-}$ mice had substantially wider villi (Figure 4-10 C). These statistical analyses show that there is a difference between the *Mmp17*$^{+/+}$ and *Mmp17*$^{-/-}$ mice, further indicating an impaired regeneration response in the mice lacking *Mmp17* expression.

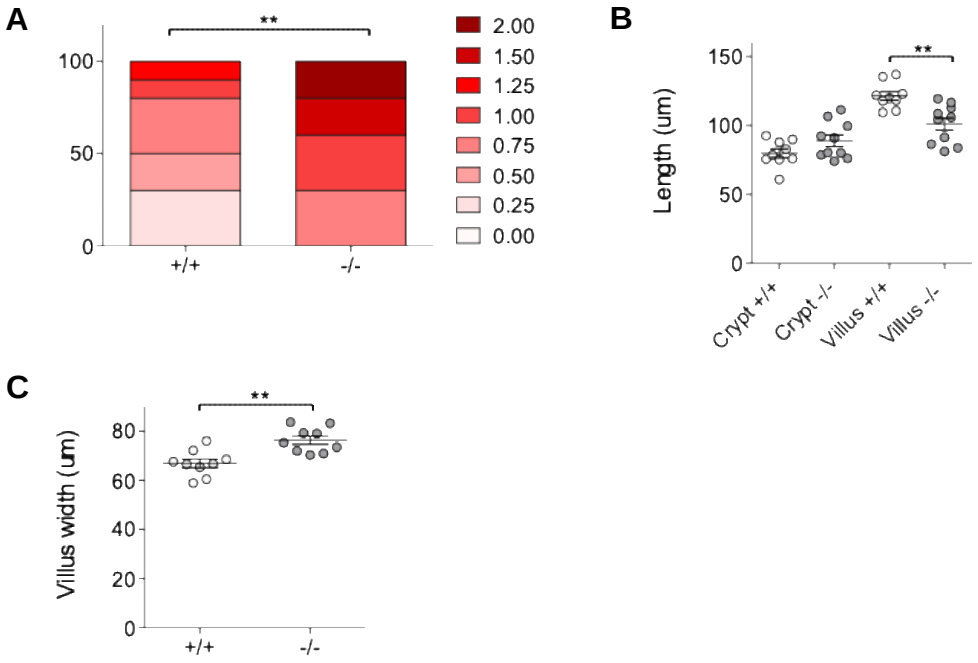

Figure 4-10: *Mmp17*$^{-/-}$ shows significant impaired regeneration when combining both experiments. (**A**) Blind injury score in *Mmp17*$^{+/+}$ and *Mmp17*$^{-/-}$ ileum 3 days post-irradiation. (**B**) Average crypt and villus length in *Mmp17*$^{+/+}$ and *Mmp17*$^{-/-}$ ileum 3 days post-irradiation. Approximately 20-30 crypts and villi were measured per mouse. (**C**) Average villus width in *Mmp17*$^{+/+}$ and *Mmp17*$^{-/-}$ ileum 3 days post-irradiation. Approximately 20-30 villi were measured per mouse. In (**A-**C) a n = 8 were analyzed per genotype per time point. Data were analyzed in (**A**) by unpaired t-test (p** < 0.01), in **(B)** by one-way ANOVA followed by a Bonferroni's multiple comparisons test (p** < 0.01) and in **(C)** by unpaired t-test (p** < 0.01). Error bars in **(B-C)** mean ± SEM.

4.4 *Mmp17*$^{-/-}$ mice displays a potential decrease in proliferation at the bottom of the crypts after radiation exposure

As described earlier, radiation targets the actively dividing cells in a tissue and induce a regenerative process that triggers proliferation. To asses proliferation we stained tissue sections from *Mmp17*$^{+/+}$ and *Mmp17*$^{-/-}$ with Ki67, a marker for proliferating cells, at the different time points. It is described that right after irradiation (day 1) cells do not proliferate and a wave of proliferation is induced to aid mucosal healing during a regenerative phase (day 3 and day 6) (Withers & Elkind, 1970). After Ki67 staining we observed almost no Ki67 positive cells in the ileum 1 day after radiation exposure in both *Mmp17*$^{+/+}$ and *Mmp17*$^{-/-}$ mice (Figure 4-11). Both genotypes displayed an increase of Ki67 positive cells at day 3, indicating that the surviving cell were proliferating. These proliferative cells were localized along the sides of the crypt and almost no proliferation was observed at the bottom at this point. At day 6 post-irradiation, proliferative cells were located at the bottom of the crypt, however *Mmp17*$^{-/-}$ showed in general

to have less Ki67 positive cells at the bottom of the crypts. These observations need to be confirmed by a quantitative analysis, that at this moment is still pending.

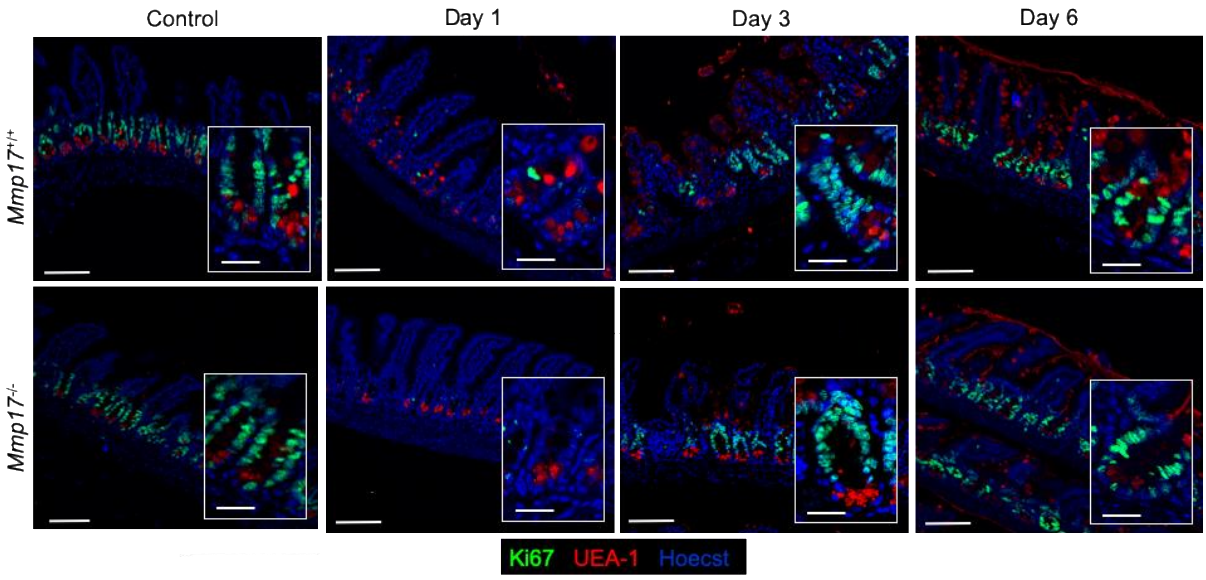

Figure 4-11: *Mmp17*$^{-/-}$ mice display a potential decrease in number of proliferative cells at the bottom of the crypts after irradiation in ileum. Representative maximal projections of confocal microscopy images of Ki67 stained ileum sections from *Mmp17*$^{+/+}$ and *Mmp17*$^{-/-}$ in control, day 1, 3 and 6 after irradiation. The nuclei in blue (Hoechst) and glycoproteins and glycolipids in red (UEA-1). Images are representative of at least a n = 3 per genotype at every time point. The scale bar indicates 100 μm and 25 μm in insets.

The colon had a similar pattern of Ki67 staining as to the one observed in the ileum. There were only a few positive Ki67 cells present 1 day after irradiation (Figure 4-12). At day 3 post-radiation exposure, there was a clear increase in the proliferation and only occurring on the sides of the crypt. This pattern of Ki67 positive cells on the side of the crypts was clearer in the colon than in the ileum. 6 days after irradiation exposure the proliferation increased. However, the same observation was made in the colon as in the ileum, were it seemed that *Mmp17*$^{-/-}$ had a lower number of proliferating cells at the bottom of the crypt, which needs to be confirmed by a pending quantitative analysis.

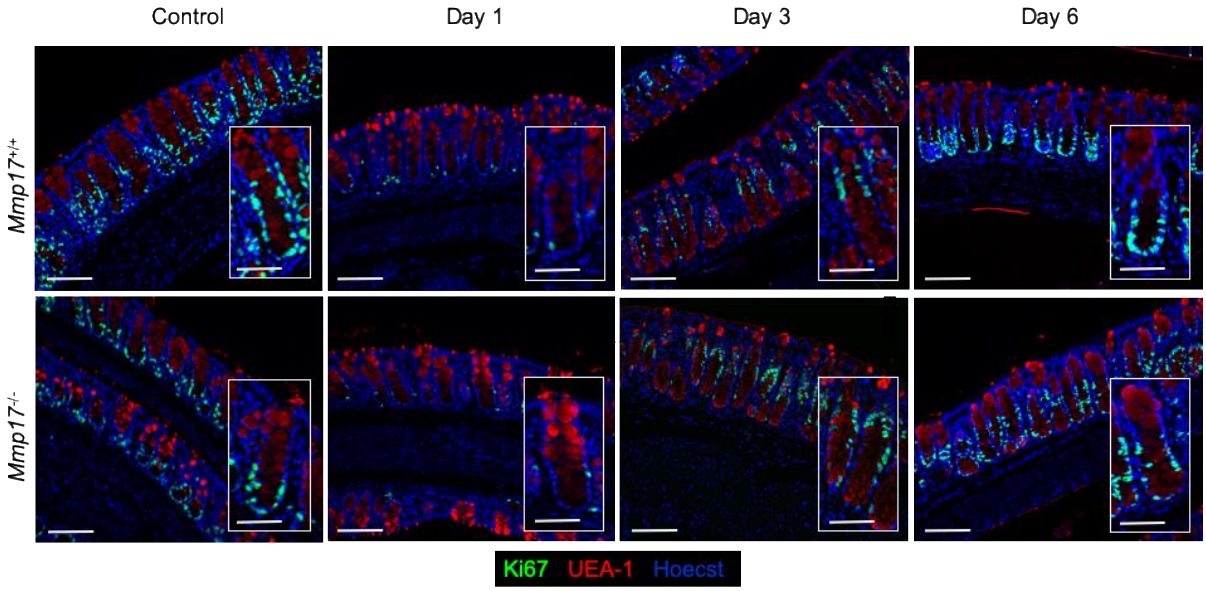

Figure 4-12: *Mmp17*$^{-/-}$ mice display a potential decrease in number of proliferative cells at the bottom of the crypts after irradiation in colon. Representative maximal projections of confocal microscopy images of Ki67 stained colon sections from *Mmp17*$^{+/+}$ and *Mmp17*$^{-/-}$ in control, day 1, 3 and 6 after irradiation. The nuclei in blue (Hoechst) and glycoproteins and glycolipids in red (UEA-1). Images are representative of at least a n = 3 per genotype at every time point. The scale bar indicates 100 μm and 50 μm in insets.

4.5 No difference in apoptosis after irradiation

As shown previously in Figure 4-2, both the ileum and colon showed positive CAS3 cells at the bottom of the crypt, indicating that the actively cycling ISCs are going through apoptosis. However, we wanted to explore if the lack of MMP17 could affect the apoptotic response at the various time points. CAS3 staining showed positive cells in both the ileum and the colon. In both tissues, CAS3 positive cells were only found at the bottom of the crypt at day 1 after radiation exposure, indicating that MMP17 does not affect the apoptotic response. (Figure 4-13 for ileum and Figure 4-14 for colon). However, these observations need to be validated by a quantitative analysis, which is still pending

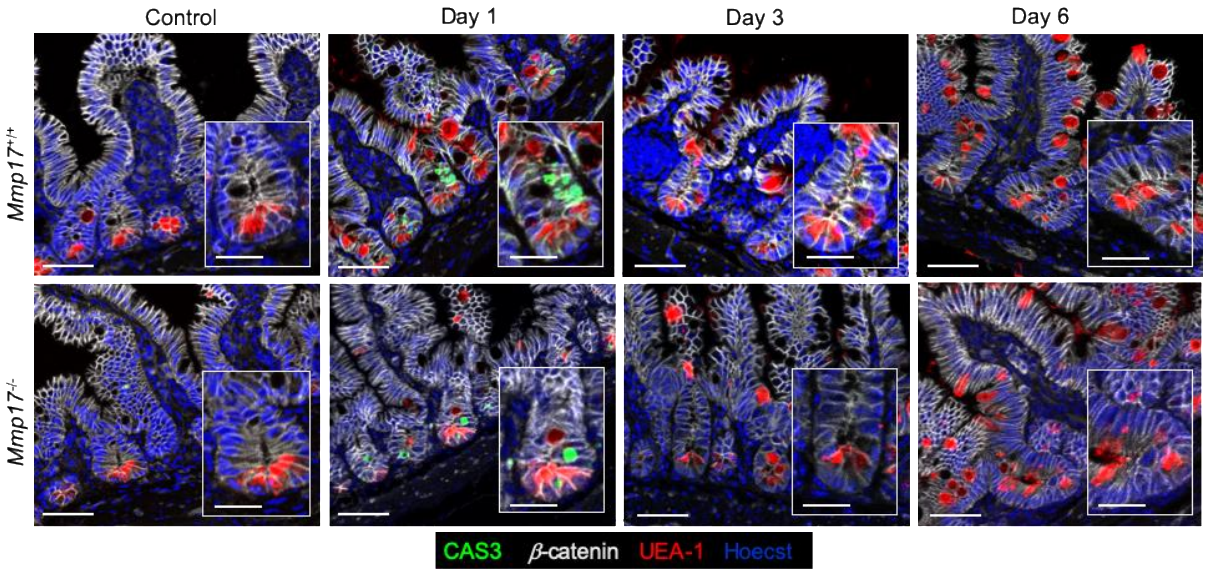

Figure 4-13: Same amount of apoptotic cells were observed 1 day after irradiation in *Mmp17*$^{+/+}$ and *Mmp17*$^{-/-}$ in ileum. Representative maximal projections of confocal microscopy images of Cleaved Caspase-3 (CAS3) stained ileum sections from *Mmp17*$^{+/+}$ and *Mmp17*$^{-/-}$ in control, day 1, 3 and 6 after irradiation. The nuclei in blue (Hoechst), glycoproteins and glycolipids in red (UEA-1) and β-catenin in white. Images are representative of at least a n = 3 per genotype at every time point. The scale bar indicates 50 μm and 25 μm in insets.

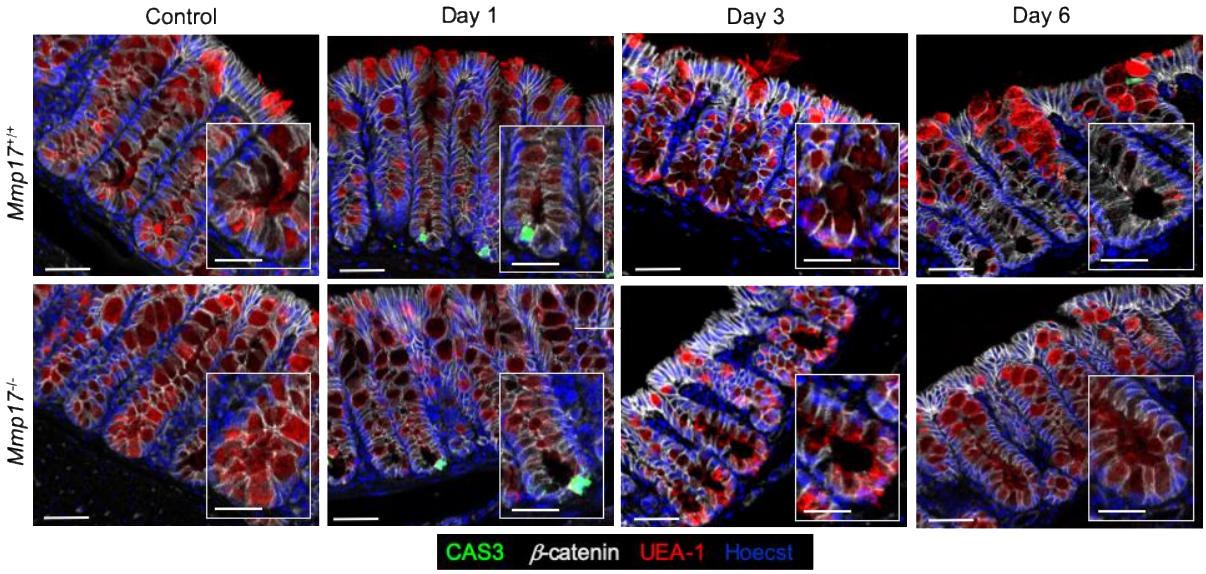

Figure 4-14: Same amount of apoptotic cells were observed 1 day after irradiation in *Mmp17*$^{+/+}$ and *Mmp17*$^{-/-}$ in colon. Representative maximal projections of confocal microscopy images of Cleaved Caspase-3 (CAS3) stained colon sections from *Mmp17*$^{+/+}$ and *Mmp17*$^{-/-}$ in control, day 1, 3 and 6 after irradiation. The nuclei in blue (Hoechst), glycoproteins and glycolipids in red (UEA-1) and β-catenin in white. Images are representative of at least a n = 3 per genotype at every time point. The scale bar indicates 50 μm and 25 μm in insets.

4.6 The lack of MMP17 alters the expression of ISC marker *Olfm4*

As highlighted earlier, irradiation will damage the ISCs at the bottom of the crypt. It was therefore essential to look into the changes in the levels of the ISCs after irradiation and to investigate if mice lacking MMP17 had altered levels of ISCs. This was done by using ISH with an *Olfm4* probe. *Oflm4* is a specific marker for the active stem cells in the crypt in the small intestine. At homeostatic conditions in the control, there was a noticeable difference in the levels of positive *Olfm4* expression (corroborating previous unpublished results of the group) (Figure 4-15 A). The positive *Olfm4* staining area was then quantified, and showed no significant difference in control, but it was a clear trend of lower *Olfm4* levels in *Mmp17*$^{-/-}$ mice (Figure 4-15 B). After irradiation, almost all *Olfm4* expression was lost, indicative of ISCs death induced by irradiation (Figure 4-15 A and B). At day 3 post-irradiation there was a small recovery in the levels of *Olfm4* expression, but due to technical difficulties, only a n = 2 and n =1 were analyzed at this timepoint. 6 days after radiation exposure, both *Mmp17*$^{+/+}$ and *Mmp17*$^{-/-}$ mice showed an increase in the levels of *Olfm4,* that even seemed to exceed the initial levels. (Figure 4-15 B).

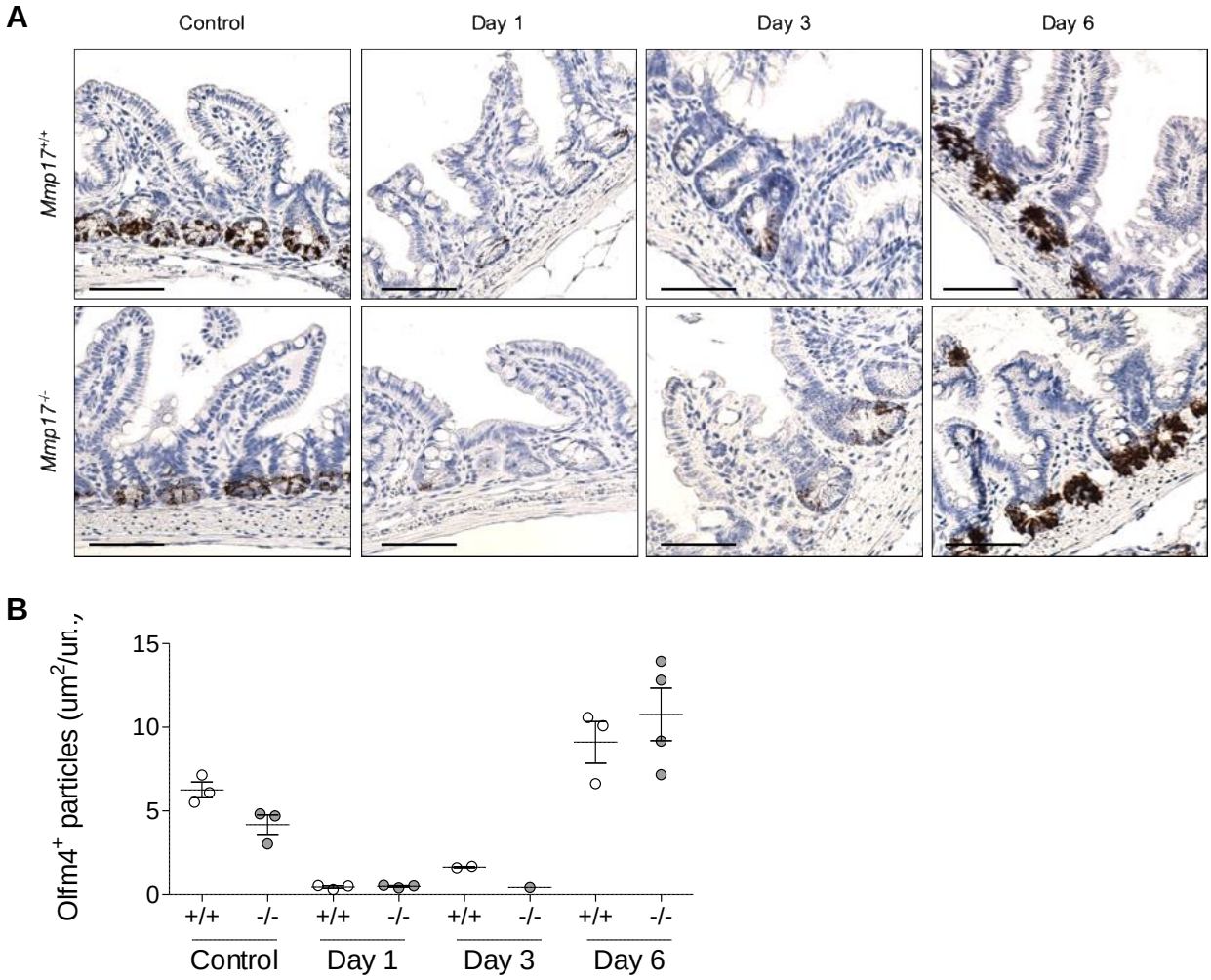

Figure 4-15: Stem cell marker *Olfm4* shows reduced ISCs after irradiation and a possible decrease in ISC number in *Mmp17*$^{-/-}$ mice. (**A**) Representative images of ISH *Olfm4* stained sections from *Mmp17*$^{+/+}$ and *Mmp17*$^{-/-}$ in ileum control and 1, 3 and 6 days after irradiation. The *Olfm4* is shown in brown and the nuclei in blue. Images are representative for at least a n = 1 per genotype per time point. The scale bar indicates 100 μm. (**B**) Average area of positive *Olfm4* particles from *Mmp17*$^{+/+}$ and *Mmp17*$^{-/-}$ in ileum, prior to irradiation and 1, 2 and 6 days after irradiation. Data were normalized to the length of the area quantified. At least a n = 1 were quantified per genotype per time point. Error bars in (**B**) present mean ± SEM and data were analyzed by a one-way ANOVA followed by Bonferroni's multiple comparisons test.

5 Discussion

The development of the *Mmp17*$^{-/-}$ strain (Rikimaru et al., 2007) enabled us to study the function of this protein *in vivo* in the intestine. Our data demonstrated that mice lacking *Mmp17* expression showed altered tissue architecture and more damage in the ileum 3 and 6 days after irradiation, compared to mice expressing *Mmp17*. In addition, it was observed a potential altered proliferation pattern 6 days after radiation in both ileum and colon and a trend of lower expression of an ISC marker in ileum during homeostasis in *Mmp17*$^{-/-}$ mice.

MMPs play an important role in degradation and remodeling of the ECM, which in the intestine makes up the structural niche around ISCs. The structural niche is produced by surrounding cells in the lamina propria, including the SMCs of the muscularis mucosae. These SMCs, together with the SMCs of the muscularis externa, specifically express MMP17, a protease identified to be involved in several pathologies and cancers. Due to the close proximity of the muscularis mucosae to the intestinal crypt, it is easy to hypothesize that this protein may impact the ISC niche and thereby their function. Earlier unpublished work from our group did not detect any structural or cellular differences in homeostasis in *Mmp17*$^{-/-}$ mice, except for decreased staining of two ISC markers. This illustrates that under homeostatic conditions, the intestine is able to cope with the loss of ISCs, which have been demonstrated by another study as well (Tian et al., 2011). It is therefore necessary to challenge the homeostatic conditions with induction of an injury to evaluate the effect of less ISCs. Our group decided to challenge the system through a DSS injury model, which causes an acute inflammatory injury in the colon. After DSS the *Mmp17*$^{-/-}$ mice displayed impaired epithelial regeneration and proliferation compared to *Mmp17*$^{+/+}$ mice (unpublished data).

This study further demonstrates the possible role of MMP17 in the regeneration process after intestinal injury caused by irradiation. The ileum in *Mmp17*$^{-/-}$ mice displayed sustained damage 3 and 6 days post-irradiation, in addition to wider and longer villi. This indicates that mice lacking MMP17 are unable to regenerate properly. Since it has been reported that the colon is more resistant to radiation induced damage (Hua et al., 2017), it was expected to find lower levels of structural alterations and damage in this tissue, which proved to be the case in our study. Increasing the radiation dose might have caused a stronger phenotype in the colon and highlighted the possible role of MMP17. However, this is not very plausible as a higher radiation dose would have induced an acute irradiation syndrome and led to major organ failure.

However, the colon was in some way affected by the irradiation, clearly shown by the reduction of $Ki67^+$ cells in the crypt. Furthermore, 6 days after irradiation in both the ileum and colon, *Mmp17*$^{-/-}$ mice displayed what looked like a decreased number of $Ki67^+$ cells at the bottom of the crypt compared to the crypts of *Mmp17*$^{+/+}$ mice. The number of proliferative cells and their pattern need to be verified in both ileum and colon, through further quantifications and analysis. However, this might indicate a possible role of MMP17 in regulation of proliferation at the bottom of the crypt after radiation exposure.

Our study suggests an additional role of MMP17 in the regulation of ISCs during homeostasis, where mice lacking MMP17 showed a trend of lower levels of the ISC marker *Olfm4* in the small intestine. These data are supported by earlier unpublished data in our group, where *Mmp17*$^{-/-}$ mice showed lower levels of *Lgr5*$^+$ in small intestine and colon and lower levels of *Olfm4* in the small intestine. However, it is important to notice that the quantification in this study measured the positive area of *Olfm4* staining. Therefore, the lower levels in *Mmp17*$^{-/-}$ mice can be caused by two scenarios; it contains less ISCs or it contains the same amount of ISCs, but it expresses a lower amount of *Olfm4* mRNA.

Considering the difference in *Olfm4* expression during homeostasis, it was expected that this difference would remain after irradiation, however this was not the case. For day 3 it was impossible to determine a difference between *Mmp17*$^{+/+}$ and *Mmp17*$^{-/-}$ mice, due to a low sample size as a result of technical difficulties. Surprisingly, 6 days after radiation exposure the *Olfm4* expression drastically increased in both genotypes compared to initial levels. A possible explanation for this could be that the ISCs at day 6 have originated from other epithelial cells in the crypt and that these are independent on the presence of MMP17. This is supported by the fact that epithelial cells have shown to be able to de-differentiate and replenish the ISCs pool under various circumstances (Asfaha et al., 2015; Buczacki et al., 2013; Schmitt et al., 2018; Tetteh et al., 2016; van Es et al., 2012; Yu et al., 2018).

MMP17 has been identified to be involved in several pathologies and cancers. However, newer research has also identified alteration in tissue structure and function with the lack of MMP17 in homeostasis. In a study investigating MMP17 and its role in thoracic aortic aneurysms and dissections, they found that the lack of MMP17 lead to changes in vascular SMCs morphology, proliferation and impaired SMC maturation (Martin-Alonso et al., 2015). This study also discovered several other features in vascular tissues, like altered response to injury and changes in ECM structure and composition in the absence of *Mmp17* expression (Martin-Alonso et al.,

2015). It further has been identified a role of SMCs during regeneration in the intestine and it has been proposed that myofibroblasts, which are important in tissue repair, could originate from these SMCs in the muscularis mucosae (Chivukula et al., 2014). This highlights the importance of proper SMCs function during the repair processes in the intestine following injury. It might be possible that MMP17 is involved in the SMCs function and their role in tissue repair, similar to what was reposted in vascular SMCs. MMP17 could also be responsible for cleaving substrates at the smooth muscle tissue, important for proper ISCs function. An early hypothesis by our group was that MMP17 could cleave substrates responsible for the regulation of the immune response during inflammation. However, this study puts this hypothesis into question, as mice lacking MMP17 still showed impaired regeneration after an injury that did not cause high levels of inflammation. This is further supported by unpublished data from our group, which demonstrated no difference in genes related to the immune system between *Mmp17*$^{+/+}$ and *Mmp17*$^{-/-}$ mice.

However, the hypothesis that MMP17 might cleave substrates that acts as paracrine regulators of ISCs remains promising. SMCs and myofibroblasts have been shown to express the BMP antagonist *Gremlin 1*, *Gremlin 2* and *Chordin-like 1* (Kosinski et al., 2007). These are crucial niche factors in the stem cell niche, as they oppose the BMP signaling and thereby promotes further proliferation in the crypt. A possibility is that the lack of MMP17 causes immature intestinal SMCs, which then do not provide proper expression and function of these BMP antagonists. A second possibility is that MMP17 cleaves one of these BMP antagonists and that the loss of this protease will lead altered BMP signaling in the crypt. Both possibilities will cause a disruption in the finetuned balance between proliferation and differentiation in the cryptand this disruption might explain the impaired regeneration and the altered expression of the ISC marker shown in this study.

As mentioned, the exact role of SMCs and MMP17 in the intestine under homeostatic conditions and in the repair process after damage remains unidentified. Future work in relation to MMP17 in the intestine should focus on identifying possible substrates and possible interactions in signaling pathways. A method for further investigation of MMP17 is to do RNA-sequencing followed by a gene-enrichment analysis from mucosal- and muscle tissues from *Mmp17*$^{+/+}$ and *Mmp17*$^{-/-}$ mice. This will give us an idea about altered genes in both tissues and difference between the *Mmp17*$^{+/+}$ and *Mmp17*$^{-/-}$ mice. The RNA-sequencing data might highlight alterations in certain signaling pathways or expression of specific proteins. The up-

and downregulation of certain genes can be further validated at protein level by performing western blots with antibodies against the proteins of interest. It is further possible to cultivate intestinal organoids, which are miniature three-dimensional structures of intestinal epithelial cells, that resemble the *in vivo* organization (Sato et al., 2009), and co-culture these organoids with muscle cells. This will make it possible to decipher the different factors the muscle cells release in the ISCs niche, which can together with the RNA sequencing data give a clearer picture of possible signaling pathways and substrates for MMP17.

Most of the methodology in this study is based on histological techniques, which provide an accurate visible description of structures and chemistry in living tissues from an organism. However, this method is a subject to human errors during both preparation and analysis of tissue slides. Because of this, certain precautions were taken; all IF stainings included negative controls, to eliminate the possibility of unspecific binding by the secondary antibodies applied. The assessment of damage was performed and scored blind, by a second researcher, to exclude the possibility of human bias. In addition, several parameters in the injury score were measured to validate the results, including the length of crypts and length and width of villi. Besides this, the main limitation of this investigation was the lack of time, which hindered the scope of analyzes and repetition of certain experiments. To strengthen the observed phenotype in *Mmp17*$^{-/-}$ ileum, it would have been useful to check the same parameters in the duodenum and jejunum of the small intestine. Under optimal circumstances, the ISH would be repeated for all time points with an increased sample size, to determine if there are any significant differences between *Olfm4* expression in *Mmp17*$^{+/+}$ and *Mmp17*$^{-/-}$ mice. In addition, it would be ideal to include the ISCs marker *Lgr5*$^{+}$, since this is a marker expressed by both the small intestine and colon. It should be mentioned that there was performed an additional *Olfm4* IF staining to confirm and validate the findings in the ISH, but due to time constrictions this staining was not analyzed and therefore not included. As previously mentioned, quantifications of both Ki67 and CAS3 should be completed to make sure validated conclusions can be made upon these different stainings.

6 Conclusion

We have demonstrated in this study a role of MMP17 in intestinal regeneration following the loss of ISCs caused by radiation exposure. This was shown through impaired regeneration, in the form of sustained damage and alterations in tissue architecture, in mice lacking MMP17. It was further suggested a possible role for MMP17 in the regulation of proliferation during regeneration and also in regulation of ISCs during homeostasis. However, these data need to be further validated. Furthermore, since the irradiation injury used in this study causes less inflammation, the possibility of MMP17 cleaving factors important for regulation of the immune system following injury can be dismissed. However further work is needed to pinpoint the role of MMP17 in the intestine, and future work should focus on identifying its substrates and which signaling pathways it might regulate. A better understanding of MMP17 is important, as this protease can be a promising target in gastrointestinal diseases and cancers.

References

Alexandre, C., Baena-Lopez, A., & Vincent, J. P. (2014). Patterning and growth control by membrane-tethered Wingless. *Nature, 505*(7482), 180-185. doi:10.1038/nature12879

Allaire, J. M., Crowley, S. M., Law, H. T., Chang, S. Y., Ko, H. J., & Vallance, B. A. (2018). The Intestinal Epithelium: Central Coordinator of Mucosal Immunity. *Trends Immunol, 39*(9), 677-696. doi:10.1016/j.it.2018.04.002

Asfaha, S., Hayakawa, Y., Muley, A., Stokes, S., Graham, T. A., Ericksen, R. E., . . . Wang, T. C. (2015). Krt19(+)/Lgr5(-) Cells Are Radioresistant Cancer-Initiating Stem Cells in the Colon and Intestine. *Cell Stem Cell, 16*(6), 627-638. doi:10.1016/j.stem.2015.04.013

Ayabe, T., Satchell, D. P., Pesendorfer, P., Tanabe, H., Wilson, C. L., Hagen, S. J., & Ouellette, A. J. (2002). Activation of Paneth cell alpha-defensins in mouse small intestine. *J Biol Chem, 277*(7), 5219-5228. doi:10.1074/jbc.M109410200

Barker, N. (2014). Adult intestinal stem cells: critical drivers of epithelial homeostasis and regeneration. *Nat Rev Mol Cell Biol, 15*(1), 19-33. doi:10.1038/nrm3721

Barker, N., van Es, J. H., Kuipers, J., Kujala, P., van den Born, M., Cozijnsen, M., . . . Clevers, H. (2007). Identification of stem cells in small intestine and colon by marker gene Lgr5. *Nature, 449*(7165), 1003-1007. doi:10.1038/nature06196

Batlle, E., Henderson, J. T., Beghtel, H., van den Born, M. M., Sancho, E., Huls, G., . . . Clevers, H. (2002). Beta-catenin and TCF mediate cell positioning in the intestinal epithelium by controlling the expression of EphB/ephrinB. *Cell, 111*(2), 251-263.

Bjerknes, M., & Cheng, H. (2001). Modulation of specific intestinal epithelial progenitors by enteric neurons. *Proc Natl Acad Sci U S A, 98*(22), 12497-12502. doi:10.1073/pnas.211278098

Blaha, M. D., & Leon, L. R. (2008). Effects of indomethacin and buprenorphine analgesia on the postoperative recovery of mice. *J Am Assoc Lab Anim Sci, 47*(4), 8-19.

Blanco, M. J., Rodriguez-Martin, I., Learte, A. I. R., Clemente, C., Montalvo, M. G., Seiki, M., . . . Sanchez-Camacho, C. (2017). Developmental expression of membrane type 4-matrix metalloproteinase (Mt4-mmp/Mmp17) in the mouse embryo. *PLoS One, 12*(9), e0184767. doi:10.1371/journal.pone.0184767

Blanpain, C., Mohrin, M., Sotiropoulou, P. A., & Passegue, E. (2011). DNA-damage response in tissue-specific and cancer stem cells. *Cell Stem Cell, 8*(1), 16-29. doi:10.1016/j.stem.2010.12.012

Bloemendaal, A. L., Buchs, N. C., George, B. D., & Guy, R. J. (2016). Intestinal stem cells and intestinal homeostasis in health and in inflammation: A review. *Surgery, 159*(5), 1237-1248. doi:10.1016/j.surg.2016.01.014

Booth, C., Tudor, G., Tudor, J., Katz, B. P., & MacVittie, T. J. (2012). Acute gastrointestinal syndrome in high-dose irradiated mice. *Health Phys, 103*(4), 383-399.

Breault, D. T., Min, I. M., Carlone, D. L., Farilla, L. G., Ambruzs, D. M., Henderson, D. E., . . . Hole, N. (2008). Generation of mTert-GFP mice as a model to identify and study tissue progenitor cells. *Proc Natl Acad Sci U S A, 105*(30), 10420-10425. doi:10.1073/pnas.0804800105

Brinckerhoff, C. E., & Matrisian, L. M. (2002). Matrix metalloproteinases: a tail of a frog that became a prince. *Nat Rev Mol Cell Biol, 3*(3), 207-214. doi:10.1038/nrm763

Buczacki, S. J., Zecchini, H. I., Nicholson, A. M., Russell, R., Vermeulen, L., Kemp, R., & Winton, D. J. (2013). Intestinal label-retaining cells are secretory precursors expressing Lgr5. *Nature, 495*(7439), 65-69. doi:10.1038/nature11965

Cathcart, J., Pulkoski-Gross, A., & Cao, J. (2015). Targeting Matrix Metalloproteinases in Cancer: Bringing New Life to Old Ideas. *Genes Dis, 2*(`1), 26-34. doi:10.1016/j.gendis.2014.12.002

Chabottaux, V., & Noel, A. (2007). Breast cancer progression: insights into multifaceted matrix metalloproteinases. *Clin Exp Metastasis, 24*(8), 647-656. doi:10.1007/s10585-007-9113-7

Chabottaux, V., Sounni, N. E., Pennington, C. J., English, W. R., van den Brule, F., Blacher, S., . . . Noel, A. (2006). Membrane-type 4 matrix metalloproteinase promotes breast cancer growth and metastases. *Cancer Res, 66*(10), 5165-5172. doi:10.1158/0008-5472.Can-05-3012

Chassaing, B., Aitken, J. D., Malleshappa, M., & Vijay-Kumar, M. (2014). Dextran sulfate sodium (DSS)-induced colitis in mice. *Curr Protoc Immunol, 104*, Unit 15.25. doi:10.1002/0471142735.im1525s104

Chen, X., Cho, D. B., & Yang, P. C. (2010). Double staining immunohistochemistry. *N Am J Med Sci, 2*(5), 241-245. doi:10.4297/najms.2010.2241

Cheng, H., & Leblond, C. P. (1974). Origin, differentiation and renewal of the four main epithelial cell types in the mouse small intestine V. Unitarian theory of the origin of the four epithelial cell types. *American Journal of Anatomy, 141*(4), 537-561. doi:doi:10.1002/aja.1001410407

Chiquet, M., Gelman, L., Lutz, R., & Maier, S. (2009). From mechanotransduction to extracellular matrix gene expression in fibroblasts. *Biochim Biophys Acta, 1793*(5), 911-920. doi:10.1016/j.bbamcr.2009.01.012

Chivukula, R. R., Shi, G., Acharya, A., Mills, E. W., Zeitels, L. R., Anandam, J. L., . . . Mendell, J. T. (2014). An essential mesenchymal function for miR-143/145 in intestinal epithelial regeneration. *Cell, 157*(5), 1104-1116. doi:10.1016/j.cell.2014.03.055

Clayburgh, D. R., Shen, L., & Turner, J. R. (2004). A porous defense: the leaky epithelial barrier in intestinal disease. *Lab Invest, 84*(3), 282-291. doi:10.1038/labinvest.3700050

Clemente, C., Rius, C., Alonso-Herranz, L., Martín-Alonso, M., Pollán, Á., Camafeita, E., . . . Arroyo, A. G. (2018). MT4-MMP deficiency increases patrolling monocyte recruitment to early lesions and accelerates atherosclerosis. *Nature Communications, 9*(1), 910. doi:10.1038/s41467-018-03351-4

Clements, K. M., Flannelly, J. K., Tart, J., Brockbank, S. M., Wardale, J., Freeth, J., . . . Newham, P. (2011). Matrix metalloproteinase 17 is necessary for cartilage aggrecan degradation in an inflammatory environment. *Ann Rheum Dis, 70*(4), 683-689. doi:10.1136/ard.2010.130757

Cook, D. J., & Warren, P. J. (2015). *Cellular Pathology; An Introduction to Techniques and Applications* (Third ed.). UK: Scion Publishing.

Coussens, L. M., Fingleton, B., & Matrisian, L. M. (2002). Matrix metalloproteinase inhibitors and cancer: trials and tribulations. *Science, 295*(5564), 2387-2392. doi:10.1126/science.1067100

Desmouliere, A., Chaponnier, C., & Gabbiani, G. (2005). Tissue repair, contraction, and the myofibroblast. *Wound Repair Regen, 13*(1), 7-12. doi:10.1111/j.1067-1927.2005.130102.x

Dholakia, U., Clark-Price, S. C., Keating, S. C. J., & Stern, A. W. (2017). Anesthetic effects and body weight changes associated with ketamine-xylazine-lidocaine administered to CD-1 mice. *PLoS One, 12*(9), e0184911. doi:10.1371/journal.pone.0184911

Engler, A. J., Sen, S., Sweeney, H. L., & Discher, D. E. (2006). Matrix elasticity directs stem cell lineage specification. *Cell, 126*(4), 677-689. doi:10.1016/j.cell.2006.06.044

English, W. R., Puente, X. S., Freije, J. M., Knauper, V., Amour, A., Merryweather, A., . . . Murphy, G. (2000). Membrane type 4 matrix metalloproteinase (MMP17) has tumor necrosis factor-alpha convertase activity but does not activate pro-MMP2. *J Biol Chem, 275*(19), 14046-14055.

Erben, U., Loddenkemper, C., Doerfel, K., Spieckermann, S., Haller, D., Heimesaat, M. M., . . . Kühl, A. A. (2014). A guide to histomorphological evaluation of intestinal inflammation in mouse models. *Int J Clin Exp Pathol, 7*(8), 4557-4576.

Farin, H. F., Van Es, J. H., & Clevers, H. (2012). Redundant sources of Wnt regulate intestinal stem cells and promote formation of Paneth cells. *Gastroenterology, 143*(6), 1518-1529.e1517. doi:10.1053/j.gastro.2012.08.031

Fischer, A. H., Jacobson, K. A., Rose, J., & Zeller, R. (2008). Hematoxylin and eosin staining of tissue and cell sections. *CSH Protoc, 2008*, pdb.prot4986. doi:10.1101/pdb.prot4986

Gao, G., Plaas, A., Thompson, V. P., Jin, S., Zuo, F., & Sandy, J. D. (2004). ADAMTS4 (aggrecanase-1) activation on the cell surface involves C-terminal cleavage by glycosylphosphatidyl inositol-anchored membrane type 4-matrix metalloproteinase and binding of the activated proteinase to chondroitin sulfate and heparan sulfate on syndecan-1. *J Biol Chem, 279*(11), 10042-10051. doi:10.1074/jbc.M312100200

Gehart, H., & Clevers, H. (2019). Tales from the crypt: new insights into intestinal stem cells. *Nature Reviews Gastroenterology & Hepatology, 16*(1), 19-34. doi:10.1038/s41575-018-0081-y

Genander, M., Halford, M. M., Xu, N. J., Eriksson, M., Yu, Z., Qiu, Z., . . . Frisen, J. (2009). Dissociation of EphB2 signaling pathways mediating progenitor cell proliferation and tumor suppression. *Cell, 139*(4), 679-692. doi:10.1016/j.cell.2009.08.048

Gomez-Escudero, J., Moreno, V., Martin-Alonso, M., Hernandez-Riquer, M. V., Feinberg, T., Colmenar, A., . . . Arroyo, A. G. (2017). E-cadherin cleavage by MT2-MMP regulates apical junctional signaling and epithelial homeostasis in the intestine. *J Cell Sci, 130*(23), 4013-4027. doi:10.1242/jcs.203687

Gregorieff, A., Pinto, D., Begthel, H., Destree, O., Kielman, M., & Clevers, H. (2005). Expression pattern of Wnt signaling components in the adult intestine. *Gastroenterology, 129*(2), 626-638. doi:10.1016/j.gastro.2005.06.007

Gross, J., & Lapiere, C. M. (1962). Collagenolytic activity in amphibian tissues: a tissue culture assay. *Proc Natl Acad Sci U S A, 48*(6), 1014-1022.

He, X. C., Zhang, J., Tong, W. G., Tawfik, O., Ross, J., Scoville, D. H., . . . Li, L. (2004). BMP signaling inhibits intestinal stem cell self-renewal through suppression of Wnt-beta-catenin signaling. *Nat Genet, 36*(10), 1117-1121. doi:10.1038/ng1430

Hendry, J. H., & Potten, C. S. (1974). Cryptogenic cells and proliferative cells in intestinal epithelium. *Int J Radiat Biol Relat Stud Phys Chem Med, 25*(6), 583-588.

Heyman, M. (2005). Gut barrier dysfunction in food allergy. *Eur J Gastroenterol Hepatol, 17*(12), 1279-1285.

Heyman, M., & Desjeux, J. F. (2000). Cytokine-Induced Alteration of the Epithelial Barrier to Food Antigens in Disease. *Annals of the New York Academy of Sciences, 915*(1), 304-311. doi:10.1111/j.1749-6632.2000.tb05258.x

Hua, G., Wang, C., Pan, Y., Zeng, Z., Lee, S. G., Martin, M. L., . . . Kolesnick, R. (2017). Distinct Levels of Radioresistance in Lgr5(+) Colonic Epithelial Stem Cells versus Lgr5(+) Small Intestinal Stem Cells. *Cancer Res, 77*(8), 2124-2133. doi:10.1158/0008-5472.Can-15-2870

Huang, C. H., Yang, W. H., Chang, S. Y., Tai, S. K., Tzeng, C. H., Kao, J. Y., . . . Yang, M. H. (2009). Regulation of membrane-type 4 matrix metalloproteinase by SLUG contributes to hypoxia-mediated metastasis. *Neoplasia, 11*(12), 1371-1382.

Humphrey, J. D., Dufresne, E. R., & Schwartz, M. A. (2014). Mechanotransduction and extracellular matrix homeostasis. *Nat Rev Mol Cell Biol, 15*(12), 802-812. doi:10.1038/nrm3896

Hynes, R. O. (2009). The extracellular matrix: not just pretty fibrils. *Science, 326*(5957), 1216-1219. doi:10.1126/science.1176009

Itoh, Y., Kajita, M., Kinoh, H., Mori, H., Okada, A., & Seiki, M. (1999). Membrane type 4 matrix metalloproteinase (MT4-MMP, MMP-17) is a glycosylphosphatidylinositol-anchored proteinase. *J Biol Chem, 274*(48), 34260-34266.

Jakubowska, K., Pryczynicz, A., Iwanowicz, P., Niewinski, A., Maciorkowska, E., Hapanowicz, J., . . . Guzinska-Ustymowicz, K. (2016). Expressions of Matrix Metalloproteinases (MMP-2, MMP-7, and MMP-9) and Their Inhibitors (TIMP-1, TIMP-2) in Inflammatory Bowel Diseases. *Gastroenterol Res Pract, 2016*, 2456179. doi:10.1155/2016/2456179

Kim, C. K., Yang, V. W., & Bialkowska, A. B. (2017). The Role of Intestinal Stem Cell in Epithelial Regeneration Following Radiation-Induced Gut Injury. *Cyrr Stem Cell Rep, 3*(4), 320-332. doi:10.1007/s40778-017-0103-7

Kim, S. W., Roh, J., & Park, C. S. (2016). Immunohistochemistry for Pathologists: Protocols, Pitfalls, and Tips. *J Pathol Transl Med, 50*(6), 411-418. doi:10.4132/jptm.2016.08.08

Klein, E. A., Yin, L., Kothapalli, D., Castagnino, P., Byfield, F. J., Xu, T., . . . Assoian, R. K. (2009). Cell-cycle control by physiological matrix elasticity and in vivo tissue stiffening. *Curr Biol, 19*(18), 1511-1518. doi:10.1016/j.cub.2009.07.069

Kosinski, C., Li, V. S., Chan, A. S., Zhang, J., Ho, C., Tsui, W. Y., . . . Chen, X. (2007). Gene expression patterns of human colon tops and basal crypts and BMP antagonists as intestinal stem cell niche factors. *Proc Natl Acad Sci U S A, 104*(39), 15418-15423. doi:10.1073/pnas.0707210104

Lewanski, C. R., & Gullick, W. J. (2001). Radiotherapy and cellular signalling. *Lancet Oncol, 2*(6), 366-370. doi:10.1016/s1470-2045(00)00391-0

Lodish, H., Berk, A., Zeipursky, S. L., Matsudaira, P., Baltimore, D., & Darnell, J. (2000). *Molecular Cell Biology* (4th ed.). New Work: W. H. Freeman.

Lu, P., Takai, K., Weaver, V. M., & Werb, Z. (2011). Extracellular matrix degradation and remodeling in development and disease. *Cold Spring Harb Perspect Biol, 3*(12). doi:10.1101/cshperspect.a005058

Mankertz, J., & Schulzke, J. D. (2007). Altered permeability in inflammatory bowel disease: pathophysiology and clinical implications. *Curr Opin Gastroenterol, 23*(4), 379-383. doi:10.1097/MOG.0b013e32816aa392

Martin-Alonso, M. (2016). *Role of the protease MT4-MMP in the arterial vasculature.* (PhD), Universidad Autónoma de Madrid, Madrid.

Martin-Alonso, M., Garcia-Redondo, A. B., Guo, D., Camafeita, E., Martinez, F., Alfranca, A., . . . Arroyo, A. G. (2015). Deficiency of MMP17/MT4-MMP proteolytic activity predisposes to aortic aneurysm in mice. *Circ Res, 117*(2), e13-26. doi:10.1161/circresaha.117.305108

Meran, L., Baulies, A., & Li, V. S. W. (2017). Intestinal Stem Cell Niche: The Extracellular Matrix and Cellular Components. *Stem Cells Int, 2017*, 7970385. doi:10.1155/2017/7970385

Merritt, A. J., Potten, C. S., Kemp, C. J., Hickman, J. A., Balmain, A., Lane, D. P., & Hall, P. A. (1994). The role of p53 in spontaneous and radiation-induced apoptosis in the gastrointestinal tract of normal and p53-deficient mice. *Cancer Res, 54*(3), 614-617.

Metcalfe, C., Kljavin, N. M., Ybarra, R., & de Sauvage, F. J. (2014). Lgr5+ stem cells are indispensable for radiation-induced intestinal regeneration. *Cell Stem Cell, 14*(2), 149-159. doi:10.1016/j.stem.2013.11.008

Milano, J., McKay, J., Dagenais, C., Foster-Brown, L., Pognan, F., Gadient, R., . . . Ciaccio, P. J. (2004). Modulation of notch processing by gamma-secretase inhibitors causes intestinal goblet cell metaplasia and induction of genes known to specify gut secretory lineage differentiation. *Toxicol Sci, 82*(1), 341-358. doi:10.1093/toxsci/kfh254

Miyoshi, H., Ajima, R., Luo, C. T., Yamaguchi, T. P., & Stappenbeck, T. S. (2012). Wnt5a potentiates TGF-beta signaling to promote colonic crypt regeneration after tissue injury. *Science, 338*(6103), 108-113. doi:10.1126/science.1223821

Montgomery, R. K., Carlone, D. L., Richmond, C. A., Farilla, L., Kranendonk, M. E., Henderson, D. E., . . . Breault, D. T. (2011). Mouse telomerase reverse transcriptase (mTert) expression marks slowly cycling intestinal stem cells. *Proc Natl Acad Sci U S A, 108*(1), 179-184. doi:10.1073/pnas.1013004108

Moolenbeek, C., & Ruitenberg, E. J. (1981). The "Swiss roll": a simple technique for histological studies of the rodent intestine. *Lab Anim, 15*(1), 57-59.

Moore-Olufemi, S. D., Padalecki, J., Olufemi, S. E., Xue, H., Oliver, D. H., Radhakrishnan, R. S., . . . Cox, C. S., Jr. (2009). Intestinal edema: effect of enteral feeding on motility and gene expression. *J Surg Res, 155*(2), 283-292. doi:10.1016/j.jss.2008.08.040

Nagase, H., & Woessner, J. F., Jr. (1999). Matrix metalloproteinases. *J Biol Chem, 274*(31), 21491-21494.

Neunlist, M., Aubert, P., Bonnaud, S., Van Landeghem, L., Coron, E., Wedel, T., . . . Galmiche, J. P. (2007). Enteric glia inhibit intestinal epithelial cell proliferation partly through a TGF-beta1-dependent pathway. *Am J Physiol Gastrointest Liver Physiol, 292*(1), G231-241. doi:10.1152/ajpgi.00276.2005

Nimri, L., Barak, H., Graeve, L., & Schwartz, B. (2013). Restoration of caveolin-1 expression suppresses growth, membrane-type-4 metalloproteinase expression and metastasis-associated activities in colon cancer cells. *Mol Carcinog, 52*(11), 859-870. doi:10.1002/mc.21927

Nouri-Aria, K. T. (2008). In situ Hybridization. *Methods Mol Med, 138*, 331-347. doi:10.1007/978-1-59745-366-0_27

Nusse, R., & Clevers, H. (2017). Wnt/beta-Catenin Signaling, Disease, and Emerging Therapeutic Modalities. *Cell, 169*(6), 985-999. doi:10.1016/j.cell.2017.05.016

Okayasu, I., Hatakeyama, S., Yamada, M., Ohkusa, T., Inagaki, Y., & Nakaya, R. (1990). A novel method in the induction of reliable experimental acute and chronic ulcerative colitis in mice. *Gastroenterology, 98*(3), 694-702.

Overall, C. M. (2002). Molecular determinants of metalloproteinase substrate specificity: matrix metalloproteinase substrate binding domains, modules, and exosites. *Mol Biotechnol, 22*(1), 51-86. doi:10.1385/mb:22:1:051

Owens, B. M., & Simmons, A. (2013). Intestinal stromal cells in mucosal immunity and homeostasis. *Mucosal Immunol, 6*(2), 224-234. doi:10.1038/mi.2012.125

Page-McCaw, A., Ewald, A. J., & Werb, Z. (2007). Matrix metalloproteinases and the regulation of tissue remodelling. *Nat Rev Mol Cell Biol, 8*(3), 221-233. doi:10.1038/nrm2125

Papke, C. L., Yamashiro, Y., & Yanagisawa, H. (2015). MMP17/MT4-MMP and thoracic aortic aneurysms: OPNing new potential for effective treatment. *Circ Res, 117*(2), 109-112. doi:10.1161/circresaha.117.306851

Paris, F., Fuks, Z., Kang, A., Capodieci, P., Juan, G., Ehleiter, D., . . . Kolesnick, R. (2001). Endothelial apoptosis as the primary lesion initiating intestinal radiation damage in mice. *Science, 293*(5528), 293-297. doi:10.1126/science.1060191

Patwari, P., Gao, G., Lee, J. H., Grodzinsky, A. J., & Sandy, J. D. (2005). Analysis of ADAMTS4 and MT4-MMP indicates that both are involved in aggrecanolysis in interleukin-1-treated bovine cartilage. *Osteoarthritis Cartilage, 13*(4), 269-277. doi:10.1016/j.joca.2004.10.023

Pei, D., & Weiss, S. J. (1995). Furin-dependent intracellular activation of the human stromelysin-3 zymogen. *Nature, 375*(6528), 244-247. doi:10.1038/375244a0

Pelham, R. J., Jr., & Wang, Y. (1997). Cell locomotion and focal adhesions are regulated by substrate flexibility. *Proc Natl Acad Sci U S A, 94*(25), 13661-13665. doi:10.1073/pnas.94.25.13661

Peterson, L. W., & Artis, D. (2014). Intestinal epithelial cells: regulators of barrier function and immune homeostasis. *Nat Rev Immunol, 14*(3), 141-153. doi:10.1038/nri3608

Peyton, S. R., & Putnam, A. J. (2005). Extracellular matrix rigidity governs smooth muscle cell motility in a biphasic fashion. *J Cell Physiol, 204*(1), 198-209. doi:10.1002/jcp.20274

Plotnikov, S. V., Pasapera, A. M., Sabass, B., & Waterman, C. M. (2012). Force fluctuations within focal adhesions mediate ECM-rigidity sensing to guide directed cell migration. *Cell, 151*(7), 1513-1527. doi:10.1016/j.cell.2012.11.034

Potten, C. S. (1977). Extreme sensitivity of some intestinal crypt cells to X and gamma irradiation. *Nature, 269*(5628), 518-521.

Potten, C. S., Hume, W. J., Reid, P., & Cairns, J. (1978). The segregation of DNA in epithelial stem cells. *Cell, 15*(3), 899-906.

Potten, C. S., Owen, G., & Booth, D. (2002). Intestinal stem cells protect their genome by selective segregation of template DNA strands. *J Cell Sci, 115*(Pt 11), 2381-2388.

Powell, A. E., Wang, Y., Li, Y., Poulin, E. J., Means, A. L., Washington, M. K., . . . Coffey, R. J. (2012). The pan-ErbB negative regulator Lrig1 is an intestinal stem cell marker that functions as a tumor suppressor. *Cell, 149*(1), 146-158. doi:10.1016/j.cell.2012.02.042

Puente, X. S., Pendas, A. M., Llano, E., Velasco, G., & Lopez-Otin, C. (1996). Molecular cloning of a novel membrane-type matrix metalloproteinase from a human breast carcinoma. *Cancer Res, 56*(5), 944-949.

Rao, N. J., & Wang, J. Y. (2010). *Regulation of Gastrointestinal Mucosal Growth*. San Rafael: Morgan & Calypool Life Sciences.

Rikimaru, A., Komori, K., Sakamoto, T., Ichise, H., Yoshida, N., Yana, I., & Seiki, M. (2007). Establishment of an MT4-MMP-deficient mouse strain representing an efficient tracking system for MT4-MMP/MMP-17 expression in vivo using beta-galactosidase. *Genes Cells, 12*(9), 1091-1100. doi:10.1111/j.1365-2443.2007.01110.x

Ross, M., & Pawlina, W. (2016). *Histology: A Text and Atlas: with Correlated Cell and Molecular Biology* (Seventh ed.). Philadelphia: Wolters Kluwer.

Rozanov, D. V., Hahn-Dantona, E., Strickland, D. K., & Strongin, A. Y. (2004). The low density lipoprotein receptor-related protein LRP is regulated by membrane type-1 matrix metalloproteinase (MT1-MMP) proteolysis in malignant cells. *J Biol Chem, 279*(6), 4260-4268. doi:10.1074/jbc.M311569200

Rozario, T., & DeSimone, D. W. (2010). The extracellular matrix in development and morphogenesis: a dynamic view. *Dev Biol, 341*(1), 126-140. doi:10.1016/j.ydbio.2009.10.026

Sancho, R., Cremona, C. A., & Behrens, A. (2015). Stem cell and progenitor fate in the mammalian intestine: Notch and lateral inhibition in homeostasis and disease. *EMBO Rep, 16*(5), 571-581. doi:10.15252/embr.201540188

Sangiorgi, E., & Capecchi, M. R. (2008). Bmi1 is expressed in vivo in intestinal stem cells. *Nat Genet, 40*(7), 915-920. doi:10.1038/ng.165

Sato, T., van Es, J. H., Snippert, H. J., Stange, D. E., Vries, R. G., van den Born, M., . . . Clevers, H. (2010). Paneth cells constitute the niche for Lgr5 stem cells in intestinal crypts. *Nature, 469*, 415. doi:10.1038/nature09637

Sato, T., Vries, R. G., Snippert, H. J., van de Wetering, M., Barker, N., Stange, D. E., . . . Clevers, H. (2009). Single Lgr5 stem cells build crypt-villus structures in vitro without a mesenchymal niche. *Nature, 459*(7244), 262-265. doi:10.1038/nature07935

Schindelin, J., Arganda-Carreras, I., Frise, E., Kaynig, V., Longair, M., Pietzsch, T., . . . Cardona, A. (2012). Fiji: an open-source platform for biological-image analysis. *Nat Methods, 9*(7), 676-682. doi:10.1038/nmeth.2019

Schmitt, M., Schewe, M., Sacchetti, A., Feijtel, D., van de Geer, W. S., Teeuwssen, M., . . . Fodde, R. (2018). Paneth Cells Respond to Inflammation and Contribute to Tissue Regeneration by Acquiring Stem-like Features through SCF/c-Kit Signaling. *Cell Rep, 24*(9), 2312-2328.e2317. doi:10.1016/j.celrep.2018.07.085

Serra, S., & Jani, P. A. (2006). An approach to duodenal biopsies. *J Clin Pathol, 59*(11), 1133-1150. doi:10.1136/jcp.2005.031260

Silosi, I., Boldeanu, M. V., Mogoanta, S. S., Ghilusi, M., Cojocaru, M., Biciusca, V., . . . Turculeanu, A. (2014). Matrix metalloproteinases (MMP-3 and MMP-9) implication in the pathogenesis of inflammatory bowel disease (IBD). *Rom J Morphol Embryol, 55*(4), 1317-1324.

Sohail, A., Sun, Q., Zhao, H., Bernardo, M. M., Cho, J. A., & Fridman, R. (2008). MT4-(MMP17) and MT6-MMP (MMP25), A unique set of membrane-anchored matrix metalloproteinases: properties and expression in cancer. *Cancer Metastasis Rev, 27*(2), 289-302. doi:10.1007/s10555-008-9129-8

Srichai, M. B., Colleta, H., Gewin, L., Matrisian, L., Abel, T. W., Koshikawa, N., . . . Zent, R. (2011). Membrane-type 4 matrix metalloproteinase (MT4-MMP) modulates water homeostasis in mice. *PLoS One, 6*(2), e17099. doi:10.1371/journal.pone.0017099

Sternlicht, M. D., & Werb, Z. (2001). How matrix metalloproteinases regulate cell behavior. *Annu Rev Cell Dev Biol, 17*, 463-516. doi:10.1146/annurev.cellbio.17.1.463

Stzepourginski, I., Nigro, G., Jacob, J. M., Dulauroy, S., Sansonetti, P. J., Eberl, G., & Peduto, L. (2017). CD34+ mesenchymal cells are a major component of the intestinal stem cells niche at homeostasis and after injury. *Proc Natl Acad Sci U S A, 114*(4), E506-e513. doi:10.1073/pnas.1620059114

Takeda, N., Jain, R., LeBoeuf, M. R., Wang, Q., Lu, M. M., & Epstein, J. A. (2011). Interconversion between intestinal stem cell populations in distinct niches. *Science, 334*(6061), 1420-1424. doi:10.1126/science.1213214

Takeuchi, K., Maiden, L., & Bjarnason, I. (2004). Genetic aspects of intestinal permeability in inflammatory bowel disease. *Novartis Found Symp, 263*, 151-158; discussion 159-163, 211-158.

Tetteh, P. W., Basak, O., Farin, H. F., Wiebrands, K., Kretzschmar, K., Begthel, H., . . . Clevers, H. (2016). Replacement of Lost Lgr5-Positive Stem Cells through Plasticity of Their Enterocyte-Lineage Daughters. *Cell Stem Cell, 18*(2), 203-213. doi:10.1016/j.stem.2016.01.001

Thorn, K. (2016). A quick guide to light microscopy in cell biology. *Mol Biol Cell, 27*(2), 219-222. doi:10.1091/mbc.E15-02-0088

Tian, H., Biehs, B., Warming, S., Leong, K. G., Rangell, L., Klein, O. D., & de Sauvage, F. J. (2011). A reserve stem cell population in small intestine renders Lgr5-positive cells dispensable. *Nature, 478*(7368), 255-259. doi:10.1038/nature10408

Truong, A., Yip, C., Paye, A., Blacher, S., Munaut, C., Deroanne, C., . . . Sounni, N. E. (2016). Dynamics of internalization and recycling of the prometastatic membrane type 4 matrix metalloproteinase (MT4-MMP) in breast cancer cells. *Febs j, 283*(4), 704-722. doi:10.1111/febs.13625

van Es, J. H., Sato, T., van de Wetering, M., Lyubimova, A., Yee Nee, A. N., Gregorieff, A., . . . Clevers, H. (2012). Dll1+ secretory progenitor cells revert to stem cells upon crypt damage. *Nat Cell Biol, 14*(10), 1099-1104. doi:10.1038/ncb2581

van Es, J. H., van Gijn, M. E., Riccio, O., van den Born, M., Vooijs, M., Begthel, H., . . . Clevers, H. (2005). Notch/gamma-secretase inhibition turns proliferative cells in intestinal crypts and adenomas into goblet cells. *Nature, 435*(7044), 959-963. doi:10.1038/nature03659

Van Landeghem, L., Chevalier, J., Mahé, M. M., Wedel, T., Urvil, P., Derkinderen, P., . . . Neunlist, M. (2011). Enteric glia promote intestinal mucosal healing via activation of focal adhesion kinase and release of proEGF. *Am J Physiol Gastrointest Liver Physiol, 300*(6), G976-987. doi:10.1152/ajpgi.00427.2010

VanDussen, K. L., & Samuelson, L. C. (2010). Mouse atonal homolog 1 directs intestinal progenitors to secretory cell rather than absorptive cell fate. *Dev Biol, 346*(2), 215-223. doi:10.1016/j.ydbio.2010.07.026

Verma, R. P., & Hansch, C. (2007). Matrix metalloproteinases (MMPs): chemical-biological functions and (Q)SARs. *Bioorg Med Chem, 15*(6), 2223-2268. doi:10.1016/j.bmc.2007.01.011

Wagers, A. J., & Weissman, I. L. (2004). Plasticity of adult stem cells. *Cell, 116*(5), 639-648.

Wang, Y., Johnson, A. R., Ye, Q. Z., & Dyer, R. D. (1999). Catalytic activities and substrate specificity of the human membrane type 4 matrix metalloproteinase catalytic domain. *J Biol Chem, 274*(46), 33043-33049.

Welberg, L. A., Kinkead, B., Thrivikraman, K., Huerkamp, M. J., Nemeroff, C. B., & Plotsky, P. M. (2006). Ketamine-xylazine-acepromazine anesthesia and postoperative recovery in rats. *J Am Assoc Lab Anim Sci, 45*(2), 13-20.

Whittaker, M., Floyd, C. D., Brown, P., & Gearing, A. J. (1999). Design and therapeutic application of matrix metalloproteinase inhibitors. *Chem Rev, 99*(9), 2735-2776.

Withers, H. R., Brennan, J. T., & Elkind, M. M. (1970). The response of stem cells of intestinal mucosa to irradiation with 14 MeV neutrons. *Br J Radiol, 43*(515), 796-801. doi:10.1259/0007-1285-43-515-796

Withers, H. R., & Elkind, M. M. (1970). Microcolony survival assay for cells of mouse intestinal mucosa exposed to radiation. *Int J Radiat Biol Relat Stud Phys Chem Med, 17*(3), 261-267.

Xavier, R. J., & Podolsky, D. K. (2007). Unravelling the pathogenesis of inflammatory bowel disease. *Nature, 448*(7152), 427-434. doi:10.1038/nature06005

Yip, C., Foidart, P., Noël, A., & Sounni, N. E. (2019). MT4-MMP: The GPI-Anchored Membrane-Type Matrix Metalloprotease with Multiple Functions in Diseases. *Int J Mol Sci, 20*(2). doi:10.3390/ijms20020354

Young, J., Rivière, B., Cox, C. S., Jr., & Uray, K. (2014). A mathematical model of intestinal oedema formation. *Math Med Biol, 31*(1), 1-15. doi:10.1093/imammb/dqs025

Yu, S., Tong, K., Zhao, Y., Balasubramanian, I., Yap, G. S., Ferraris, R. P., . . . Gao, N. (2018). Paneth Cell Multipotency Induced by Notch Activation following Injury. *Cell Stem Cell, 23*(1), 46-59.e45. doi:10.1016/j.stem.2018.05.002

Yui, S., Azzolin, L., Maimets, M., Pedersen, M. T., Fordham, R. P., Hansen, S. L., . . . Jensen, K. B. (2018). YAP/TAZ-Dependent Reprogramming of Colonic Epithelium Links ECM Remodeling to Tissue Regeneration. *Cell Stem Cell, 22*(1), 35-49.e37. doi:10.1016/j.stem.2017.11.001